CHALMERS
UNIVERSITY OF TECHNOLOGY

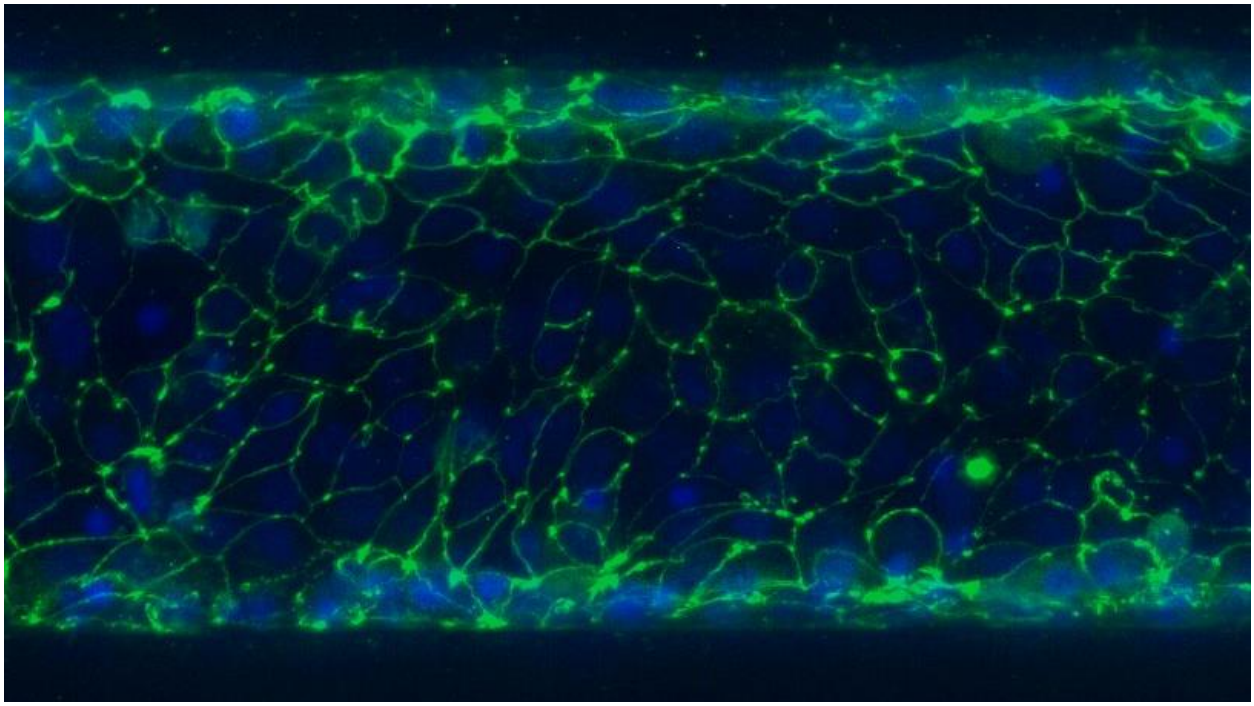

Investigating flow-related effects of Chronic Kidney Disease on renal drug toxicity in a human-derived proximal tubule microphysiological system

Master's thesis in Biotechnology

OTTO MAGNUSSON

DEPARTMENT OF PHYSICS

CHALMERS UNIVERSITY OF TECHNOLOGY
Gothenburg, Sweden 2020
www.chalmers.se

Master's thesis

Investigating flow-related effects of Chronic Kidney Disease on renal drug toxicity in a human-derived proximal tubule microphysiological system

OTTO MAGNUSSON

CHALMERS
UNIVERSITY OF TECHNOLOGY

Department of Physics
Division of Nano- and Biophysics
Chalmers University of Technology
Gothenburg, Sweden 2020

Investigating flow-related effects of Chronic Kidney Disease on renal drug toxicity in a human-derived proximal tubule microphysiological system
OTTO MAGNUSSON

Supervisor:	Tom Nieskens, CVRM Safety, Clinical Pharmacology & Safety Sciences, R&D, AstraZeneca, Gothenburg, Sweden
Supervisor:	Anna-Karin Sjögren, CVRM Safety, Clinical Pharmacology & Safety Sciences, R&D, AstraZeneca, Gothenburg, Sweden
Examiner:	Julie Gold, Department of Physics

Department of Physics
Division of Nano- and Biophysics
Chalmers University of Technology
SE-412 96 Gothenburg
Telephone +46 31 772 1000

Cover: Tight junction protein immunofluorescence stain (green) of HRPTEC cultured in a Nortis Parvivo™ chip.

Typeset in LaTeX
Printed by Chalmers Reproservice
Gothenburg, Sweden 2020

Investigating flow-related effects of Chronic Kidney Disease on renal drug toxicity in a human-derived proximal tubule microphysiological system

OTTO MAGNUSSON
Department of Physics, Chalmers University of Technology
CVRM Safety, Clinical Pharmacology & Safety Sciences, R&D, AstraZeneca, Gothenburg, Sweden

Abstract

The kidney proximal tubule is responsible for the active expulsion of drugs from the blood to the urine and is, therefore, of great importance when evaluating drug safety. Chronic kidney disease (CKD) is a major cause of reduced renal filtration function, reducing the fluid forces experienced by human renal proximal tubule eptihelial cells (HRPTEC). Developing a physiologically representative *in vitro* model for drug toxicity studies in both healthy and diseased HRPTEC would therefore be highly valuable. As CKD is a major cause of reduced renal function and may affect the function of proximal tubule cells, this thesis focused on the investigation of how flow-related aspects of chronic kidney disease affects drug transport and toxicity in HRPTEC cultured in 3D in the Nortis microphysiological system. qPCR was used to evaluate differential gene expression of drug transporters, proximal tubule and stress markers in response to flow exposure and nutrient deprivation in 3D and 2D cultured HRPTEC, alongside LDH in the supernatant and Live/Dead stain to evaluate cell viability. Phenotype by gene expression remained unchanged in the 3D proximal tubule model when exposed to a 5 week 2-fold increase to fluid shear stress (FSS) from 0.9 to 1.7 dyne/cm^2, as well as in 2D cultures exposed to orbital flow (1.9 or 5.3 dyne/cm^2) for 1 week compared to static cultures. 2D cultured cells also displayed no change to transport (P-gp) function in response to orbital flow when evaluated with Calcein-AM. Interestingly, gene expression of several drug transporters was increased in 3D HRPTEC cultures (1, 5 weeks) compared to 2D, including regained expression of OAT1 and OAT3 and upregulation of OCT2 (*SLC22A2*, 3.6 ± 1.1 fold [5 weeks]), MATE1 (*SLC47A1*, 41.3 ± 3.4 fold, 33.2 ± 13.2 fold), MATE2-K (*SLC47A2*, 71.9 ± 8.9 fold , 99.6 ± 61.7 fold) and the endocytosis receptor Megalin (*LRP2*, 46.7 ± 13.1 fold, 67.5 ± 34.1 fold). Moreover, this phenotype remained stable from 1 to 5 weeks in culture. The antibiotic polymyxin B (50 µM, 48 h) showing reduced viability to 83 ± 7.0% as evaluated by Live/Dead stain, demonstrating sensitivity to know nephrotoxicants in 3D cultured HRPTEC. Phenotype by gene expression was unaffected by nutrient and flow deprivation for 3 days. Although the aim of replicating flow related aspects of chronic kidney disease in the 3D proximal tubule model used in this study was not achieved, it was established that the 3D model displayed stable phenotype for up to five weeks with regained and significantly increased expression of drug transporter and endocytosis receptor genes when compared to 2D cultured cells. This suggests that the 3D proximal tubule model used in this study is a more physiologically relevant model for future long-term drug toxicity studies.

Keywords: chronic kidney disease, 3D *in vitro model*, drug safety, drug toxicity and transport, primary human proximal tubule cells, microfluidics, microphysiological system.

Acknowledgements

There are a lot of people I would like to thank for giving me the opportunity to write this thesis. First of all I would like to mention my supervisors Tom Nieskens and Anna-Karin Sjögren both of you have been so helpful and supportive of me throughout this entire process. Thank you both so much for trusting me and allowing me to work on this project. The rest of the team at AstraZeneca; Malin Forsgard and Liu Guanghui for helping me with laboratory work, Mikael Persson for providing me with suggestions and constructive feedback throughout the process and everyone else in CVRM and RIA Safety for making me feel welcome at AstraZeneca. Lastly, I would to thank Julie Gold for dedicating her time and being my examiner at Chalmers, providing me with tons of support and lots of great input on the project. You have all contributed so much to this project and I could not have done any of this without you.

This thesis is dedicated to my grandfather Bengt Magnusson, who was very excited to see my report when it was finished but is sadly no longer able to do so. You were always proud of me no matter what, thank you for always believing in me and for being the best grandfather anyone could ever ask for.

Otto Magnusson, Gothenburg, June 2020

Abbreviations

ABC	ATP-binding cassette
AKI	Acute kidney injury
AQP1	Aquaporin 1
BSA	Bovine serum albumin
BSA-FITC	Fluorescein isothiocyanate labeled bovine serum albumin
ciPTEC	Conditionally immortalized proximal tubule epithelial cells
CKD	Chronic Kidney disease
DMSO	Dimethyl sulfoxide
EGF	Epidermal growth factor
FCS	Fetal calf serum
GFR	Glomerular filtration rate
HC	Hydrocortisone
HRPTEC	Human renal proximal tubular epithelial cells
I3	Tri-iodothyronine
ITS	Insulin-transferrin-sodium selenite media supplement
LDH	Lactate dehydrogenase
LMW	Low molecular weight
MATE	Multidrug and toxin extrusion protein
MPS	Microphysiological system
MRP4	Multidrug resistance protein 4
NT	Noise tolerance
OAT	Organic anion transporter
OCT	Organic cation transporter
P-gp	P-glycoprotein
PDMS	Polydimethylsiloxane
PFA	Paraformaldehyde
SFM	Serum free medium
SLC	Solute carrier
ZO-1	Tight junction protein 1

Contents

List of Figures

List of Tables

1. Introduction

To increase the efficiency of drug development AstraZeneca has implemented the 5-R strategy.[1] Among these five R's is "*Right Safety*", with the purpose of mitigating adverse effects of potentially toxic compounds by identifying them early in drug discovery and development and understanding their toxicological effects.[1] One area of key importance for studying these effects is the kidneys, as they excrete drugs and drug metabolites from the circulating blood via the urine. Understanding how disruptions in kidney function affects the expulsion of drugs from the body, can provide vital information about which drugs and doses can be considered safe, when treating patients with reduced kidney function. Chronic kidney disease (CKD) is one of the major causes of reduced kidney function in patients worldwide.[2] CKD is an umbrella term for several different conditions affecting the kidneys, but is generally defined as a gradual loss of kidney function. This results in changes to the filtration capacity of the kidneys, as the number of functional nephrons in the kidney is reduced, combined with the accumulation of fibrosis, the kidneys gradually reduce the amount of filtrate able to pass through the kidney tubules as CKD progresses. This ultimately influences the physiological forces experienced by kidney cells, most notably in the proximal tubule. As the main area for active excretion and reabsortion in the kidney, the proximal tubule is most likely to be affected by changes in renal filtration and flow rate and might, because of this, affect how the kidneys process drugs.[2–4]

This project will therefore focus on how flow-related physiological aspects of CKD, including increased and decreased fluid shear stress as well as the complete absence of flow, influences drug-toxicity in the kidney proximal tubules. To achieve an *in vitro* model that comes closer to replicating the *in vivo* environment, compared to 2D cultures, we have used a kidney microphysiological system (MPS), more commonly known as kidney-on-a-chip. This system allows us to simulate the structure of the proximal tubule as cells can be grown in a 3D tubular culture. The system also creates a luminal channel which models the proximal tubule and allows us to subject the human renal proximal tubular epithelial cells used in this study to a continuous fluid shear stress. This thesis investigates drug-induced cellular toxicity as well as transcriptional changes in HRPTEC in a kidney MPS *in vitro model*. The aim is to provide insight into how flow and fluid shear stress disruptions, which occur in CKD, may affect drug toxicity in the kidney.

1.1 Aim

The aim of this project is to evaluate the effect of altered renal flow as may be observed in CKD on the drug-sensitivity of proximal tubule epithelial cells. A microphysiological system containing human renal proximal tubular epithelial cells will be used to simulate altered renal flow and fluid shear stress in the proximal tubule, with the purpose of replicating affected flow as may be observed in CKD. Under these conditions, morphological change, cell viability, drug toxicity and gene expression of markers indicating dedifferentiation, kidney damage and fibrosis will be evaluated.

1.2 Limitations

The cells used in this model are HRPTEC grown in an epithelial layer. Although the cells are human-derived they have been cryopreserved and are at passage three when used for testing, as opposed to freshly isolated cells. Simulated symptoms will be primarily limited to CKD effects related to changes in flow, experienced by the cells as fluid shear stress. Symptoms related to proteinuria and uremic toxins will not be evaluated. The collagen I matrix used in the MPS is a simplification of the ECM found in the proximal tubule basement membrane. In addition, it is crosslinked with genipin for increased rigidity, which does not allow for expansion or contraction of the replicated tubule which may occur *in vivo*. Hypoxic conditions, which would be part of simulating ischemia, will not be evaluated as the current incubator setup does not allow for this.

2. Background

2.1 Kidney anatomy & function

The kidneys are two bean shaped organs found, in humans, on both sides of the vertebral column below the diaphragm, weighing from 115 to 170 g each.[5] The kidneys are essential for the preservation of the body's internal homeostasis. They produce hormones involved in red blood cell formation and blood pressure regulation, regulate the body's fluid status, electrolyte and acid-base balance and mediate the excretion of metabolic waste products, toxins and drugs into the urine. The functional unit of the kidney is the nephron (Figure 2.1) and in humans approximately 1 million nephrons are found in each kidney.[6] The nephron consists of the renal corpuscle and the renal tubule and connects to the kidney's collecting duct system.[5]

The renal corpuscle is made up of two subunits, the glomerulus and Bowman's capsule. The glomerulus is a dense structure of porous capillaries where the blood flowing through the kidney is ultrafiltrated through a membrane, created by specialized epithelial cells known as podocytes, into the lumen of Bowman's capsule.[5,6] The normal human glomerular filtration rate (GFR) of both kidneys is around 180 L/day. This high rate of filtration is achieved due to the fact that the kidneys receive 20-25% of the cardiac output, an unproportionally large fraction when taking into account that the kidneys make up less than 0.5% of the total body mass.[5] The glomerular filtrate contains similar concentrations of small solutes as the blood plasma it originates from. Water and solutes, which may include waste products, salts, amino acids, glucose, drugs and drug metabolites, pass through the filtration membrane and enter the tubular portion of the nephron. Large molecules (>70 kDa) like proteins and other high molecular weight compounds, as well as protein bound compounds or drugs, remain in the circulatory system as they cannot easily pass through the filtration membrane in the glomerulus.[5]

The renal tubule connects to Bowman's capsule and is comprised of several different segments including the loop of Henle, the distal tubule, the connecting tubule and the proximal tubule. Here, the glomerular filtrate is processed, the main function of the renal tubule being the reabsorbtion of fluids and solutes from the filtrate.[6] Reabsorptive and excretive transport of selected solutes takes place over the epithelium of the tubule. The nature of this transport depends on the tubular subsection. The proximal tubule is responsible for the reabsorbtion of protein and other solutes from the glomerular filtrate by means of receptor-mediated endocytosis, as well as active and passive transcellular transport of small molecules.[5]

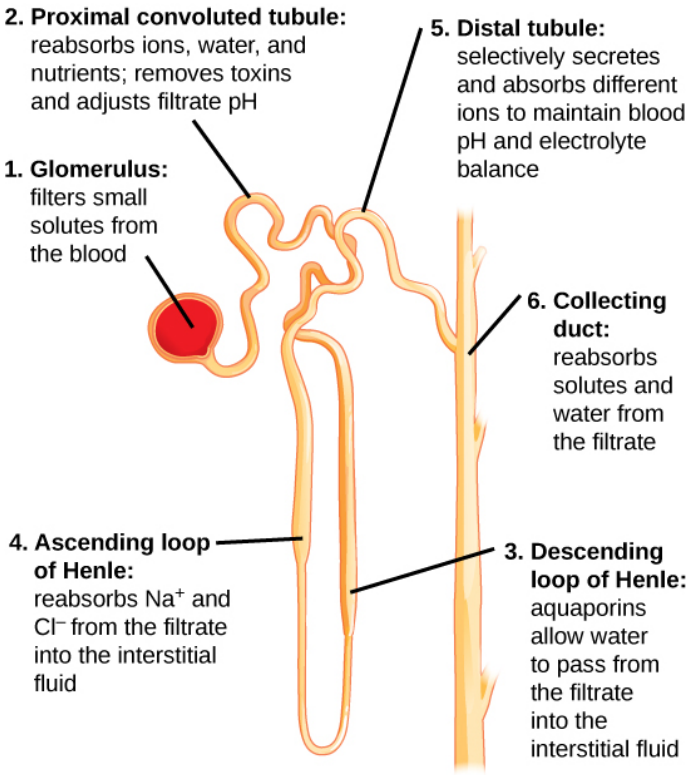

Figure 2.1: Structural schematic of the nephron with brief functional descriptions of its major components. (CNX Openstax, 2016)

2.1.1 The proximal tubule

The main location of active drug excretion in the kidney is the epithelium of the proximal tubule. Here, a large amount of trans-membrane drug-transporters (Figure 2.2) account for the transcellular transfer of drugs, metabolites and toxins from the blood to the urine as well as for the reabsorbtion of water and nutrients including proteins, glucose and amino acids.[3,4] An imbalance in the uptake and efflux capacity of the cells can cause the concentration of drugs within the epithelial cells or in the blood to increase to toxic levels.[7,4,8] This makes the epithelium of the proximal tubule especially sensitive to drug-induced nephrotoxicity.

Human renal proximal tubular epithelial cells (HRPTEC) make up the epithelial layer of the proximal tubule. These cells are highly polarized but form the least tight epithelial structure in the renal tubule, allowing paracellular transport of water.[9] In combination with high expression of the water channel protein Aquaporin 1 (AQP1) on both the apical and basolateral membrane of HRPTEC, this results in the reabsorbtion of 67% of the total water volume of the glomerular filtrate by the proximal tubule.[10,11] HRPTEC also possess large amounts of microvilli and a single primary cilium on the apical membrane, creating a dense brush border at the cell-lumen interface, increasing its surface area greatly. This provides the cells with a flow sensing mechanism as the primary cilia, when activated by flow, mediate the uptake of Ca^{2+} from the lumen.[12] This initiates a phosphorylation cascade in the proximal tubule cells resulting in protein activation and regulation of a large number of genes.[12] The microvilli are more closely linked to receptor mediated endocytosis, as pits in the cellular membrane found between the microvilli contain high concentrations

of megalin (*LRP2*) and cubilin (*CUBN*).[13] These two proteins form a receptor complex on the apical membrane that mediates the endocytosis of a wide range of ligands.[14] Megalin belongs to the low density lipoprotein-receptor family and is a crucial component in the reabsorption of albumin and other proteins from the glomerular filtrate. Megalin knockout mice exhibit elevated concentrations of albumin (albuminuria) and other low molecular weight (LMW) proteins in the urine.[14] Megalin has also been described to mediate the reabsorption of polymyxin B, gentamicin and other aminoglycoside antibiotics from the urine.[15]

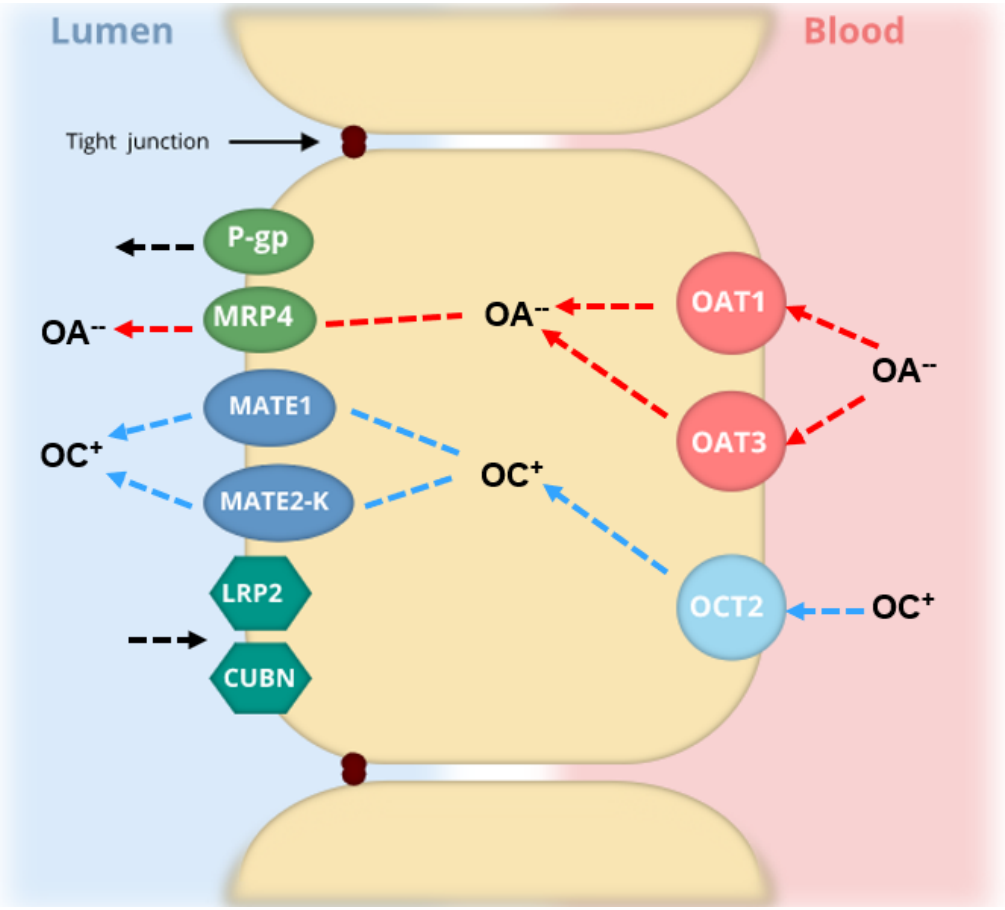

Figure 2.2: Illustration of transport protein localization in HRPTEC. With illustrations of transcellular transport of organic anions (OA^-) and cations (OC^+).

The proximal tubule expresses dedicated uptake and efflux transport proteins on both the apical and basolateral membranes of the proximal tubule. Transport proteins located on the basolateral membrane facilitate uptake of drugs from the internal circulation into the proximal tubule epithelium, and make up the first transport step in the process of urinary excretion.[16] These include organic anion transporters 1 (OAT1, *SLC22A6*) and 3 (OAT3, *SLC22A8*) and organic cation transporter 2 (OCT2, *SLC22A2*), see Figure 2.2.[16] These uptake transporters belong to the solute carrier (SLC) transporter family, meaning active transport against a concentration gradient is driven by co-transport of another substrate with its concentration gradient. OAT1 and OAT3 are polyspecific antiporters that transfer mainly anionic xenobiotics, metabolites and drugs from the blood in exchange for a-ketoglutarate.[16] OCT2 handles mostly cationic substrates but has also been described to transport zwitterionic and anionc substrates across the basolateral membrane. It is a

facilitated diffusion transporter, driving active transport against concentration gradients by the inward-directed negative membrane potential.[17]

Transport proteins located on the apical membrane facilitate efflux of drugs from the proximal tubule epithelium into the tubule lumen. These include P-glycoprotein (P-gp, *ABCB1*), multidrug resistance protein 4 (MRP4, *ABCC4*), multidrug and toxin extrusion protein 1 (MATE1, *SLC47A1*) and 2-K (MATE2-K, *SLC47A2*), see Figure 2.2.[7,18] These efflux transporters belong to the SLC and ATP-binding cassette (ABC) family, the latter driving active transport against a concentration gradient by making use of ATP hydrolysis. The substrate overlap between these transporters is relatively high, however, MRP4 displays a high affinity for conjugated and anionic substrates while P-gp has been described to favor unconjugated and cationic substrates.[19,20]

MATE1 and MATE2-K are proton antiporters that express the highest affinity for cations.[18] MATEs use the proton gradient over the apical membrane to drive active transport, resulting from the relatively low pH (<7.4) of the proximal tubule lumen.[18] Not unlike ABC transporters, substrate overlap is high among MATE proteins, suggesting a redundancy system, although some substrates remain unique for each transporter.[18] MATE2-K is exclusively expressed in proximal tubule cells where it acts as an efflux transporter. MATE1 is expressed in a variety of tissues including liver and skeletal muscle tissue where it functions as an uptake transporter, in the proximal tubule however, this function is reversed and it instead acts as an efflux transporter.[18]

Uptake transporters work in concert with efflux transport proteins to facilitate transcellular transport of drugs (Figure 2.2), resulting in their elimination from the body. OCT2 has been described to work together with both MATE1 and MATE2-K in the excretion of cations, such as the chemotherapeutic drug cisplatin.[21] OAT1 and OAT3 work together with MRP4, in the excretion of anions, like the excretion of the antiviral tenofovir.[22]

2.2 Acute kidney injury

As a result of drug-induced damage to proximal tubule cells, their epithelial structures may lose function, detach from the basal membrane or go into apoptosis or necrosis, leading to acute kidney injury (AKI)(Figure 2.3).[23] AKI occurrence is not limited to drug-toxicity and may be caused by other factors such as trauma or a disruption of blood flow (ischemia) to the kidneys. Ischemia reperfusion injury has been closely linked to the occurrence of kidney fibrosis and the development of permanent kidney injury, where the severity of the injury is dependent on the duration of the ischemic episode.[24] Repeated instances of AKI have a cumulative effect, especially in the case of ischemia and may accelerate the development of permanent kidney injury and CKD.[24,25]

2.3 Chronic kidney disease

CKD is a multi-factorial disease with a variety of underlying causes affecting the kidneys. It is defined by the presence of kidney damage (albuminuria) or a decrease in kidney function (GFR lower than 60 ml/min per 1.73 m^2) lasting for more than three months.[2,23]

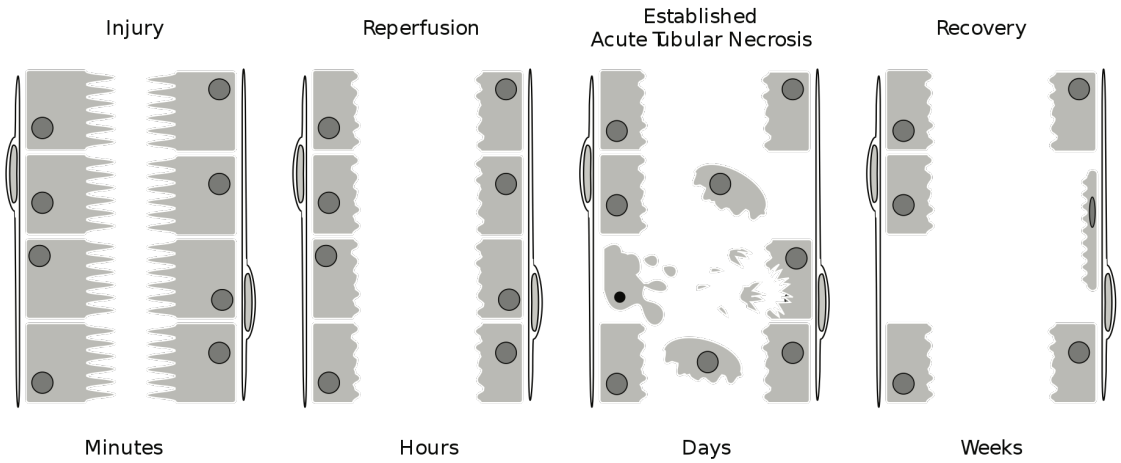

Figure 2.3: Illustration of cellular response to ischemia reperfusion injury in the proximal tubule. (ColnKurtz, 2017)

In recent years, a recommendation for the reclassification of CKD has been put forward, redefining the disease from a late-stage life-threatening condition to a more common condition of wide-ranging severity affecting a larger population.[2] It is estimated that the prevalence of CKD is 8-16% worldwide and has increased from 27th (1990) to 18th (2010) on the list of causes of total number of global deaths.[26,27] The need for knowledge of drug related complications of CKD is therefore increasingly relevant. CKD presents with a variety of symptoms, including proteinuria, systemic increases in uremic toxins as well as disturbances in the flow rate of the glomerular filtrate.

Glomerular hyperfiltration is defined as an increase in the total GFR (125-175 per 1.73 m^2) and results in an increase in fluid shear stress and tensile stress on the proximal tubule epithelium.[28] Although it is not considered a symptom of fully developed CKD, hyperfiltration is closely associated with obesity and diabetes and is thought to play an key role in the pathological development of CKD in patients with these conditions.[29,28] Glomerular hypofiltration is associated with the late stages of CKD, resulting in reduced total GFR (<60 ml/min per 1.73 m^2).[2] How this affects single nephron filtration rate is yet to be determined. It may be a result of reduced blood flow to the kidneys causing a general reduction in filtration rate for all nephrons in the kidneys.[30] It could also be the result of a decrease in the number of functional nephrons in the kidneys, as commonly seen after instances of AKI and plays a key role in the progression from AKI to CKD.[25] This reduces the total GFR but also increases the demand for increased single nephron filtration rate in the remaining functional nephrons. As CKD develops, ischemia may also increase in frequency and have more severe effects, causing further kidney injury and reduction in nephron numbers, resulting in kidney fibrosis.[25]

All conditions described above influence the amount of fluid shear stress experienced by the cells in the proximal tubule and in turn influence morphology, gene expression, transport function and drug-induced toxicity in the cells.[31,32] Investigating the possible effects of these functional changes on drug reabsorption and toxicity is therefore very important from a drug safety perspective, as it may differ from what can be seen in the healthy kidney.

2.4 Microphysiological systems

Microphysiological systems (MPS), also know as organ-on-a-chip or microfluidics systems, are *in vitro* testing platforms developed to provide a tool that comes closer to replicating the physiological environment compared to traditional 2D cultures. This is achieved by providing the cell with a similar structure to how the cells would be found *in vivo*. These include 3D culturing and exposing the cells to physiological stresses associated with their function e.g fluid shear stress for proximal tubule cells or mechanical stress for muscle cells or through a combination of these two factors.

MPS capable of simulating kidney function by replicating the epithelial layer of the proximal tubule, have been the subject of many recent studies.[33,31,34,8,35] That is why the setup chosen for this project is a 3D culture system mimicking the proximal tubule, as it is the most sensitive kidney structure and most important when evaluating toxicity.[4,8] 3D culturing also provides certain benefits compared to 2D cultures as it comes closer to replicating the conditions experienced by HRPTEC *in vivo*, including exposure to flow and tubular structure. A visual representation of how cells are cultured in the MPS system used in this project can be seen in Figure 2.4.

2.4.1 Effect of fluid shear stress on cell function

In the case of HRPTEC, exposure to flow and fluid shear stress plays an important role in replicating the *in vivo* environment, influencing the morphology, gene expression, drug transporter function and endocytosis function as well as toxicity response of the cells.[31,32,8] The morphological changes seen in HRPTEC grown in an MPS include increased cell height and an increased expression of cilia compared to cultures not exposed to flow.[31] Protein expression changes that can be seen in MPS cultured HRPTEC include increased expression of epithelial (Tight junction protein 1 [ZO-1]) and proximal tubule markers (AQP1) compared to static cultures, indicating a more mature epithelial phenotype.[31]

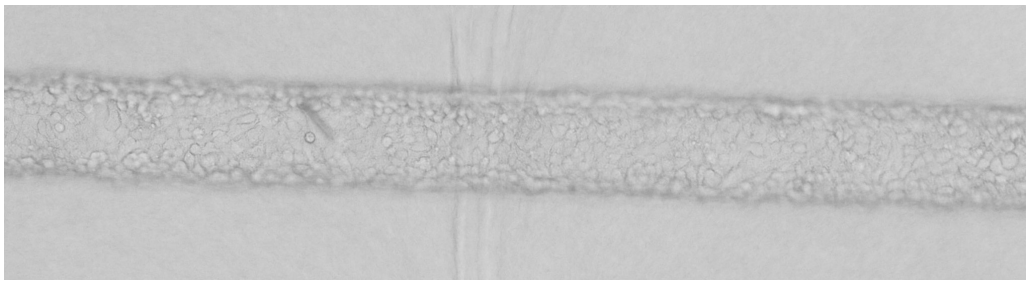

Figure 2.4: Phase contrast image of HRPTEC cultured in Nortis ParVivo™ chip. The cells are seen from a top-down perspective with cells in focus being attached to the bottom and sides of the cell culture tube, 10x magnification.

Active transport function (P-gp activity) and endocytosis function (Megalin) has also been found to be increased in human proximal tubule derived cells cultured in MPS systems compared to traditional 2D cultures.[31,36,37] Using an MPS system capable of inducing laminar flow, P-gp function was found to increase in response to flow when assayed using calcein-AM[31]. Albumin uptake has been evaluated using BSA-FITC assay on human conditionally immortalized proximal tubule epithelial cells (ciPTEC) cultured in an MPS system. Increases in flow rate (0.5 dyne/cm^2 compared to 2 dyne/cm^2) resulted in an

increase in uptake function, suggesting increased endocytic capacity in cells exposed to increased flow rates.[37] Interesting to note is that no increased gene expression of *LRP2* was detected to support functional evidence, underlining that gene expression is not always representative of cell function.[37] In addition, flow is able to change the sensitivity to cisplatin exposure in HRPTEC. Cisplatin is a well-known nephrotoxin used in chemotherapy, it is taken up by OCT2 in the basolateral membrane of the proximal tubules.[38] Cells exposed to flow were found to be less sensitive to cisplatin toxicity and recover to a greater extent than cells grown in static cultures, while toxicity was reduced upon co-incubation with OCT2 inhibitor cimetidine. Together, indicating that the 3D fluidic MPS culture might be a more relevant model for evaluating renal drug-toxicity compared to 2D cultures.[33,31,38]

2.4.2 Nortis ParVivo™ system

The Nortis ParVivo™ chip system (Figure 2.5) has been validated for several organ-on-a-chip models, including the proximal tubule.[39,8,35] The Nortis ParVivo™ chips consist of a plastic frame with an integrated glass cover slip for imaging and microscopy. The internal structure of the chips is composed of Polydimethylsiloxane (PDMS) with internal channels that permit matrix injection and medium perfusion. The matrix chamber is pre-filled with PBS and contains a glass fiber which is removed after matrix injection, creating the cell tube. The cell tube diameter is 125 µm and the tube is between 5-5.8 mm long, depending on the chip type. For this project, single, dual and triple channel chips were available for use (Figure 2.6). Single and triple channel chips only allow medium perfusion to occur along the apical membrane of the cells, while dual channel chips also allow medium perfusion on the basolateral side of the cell tube, making it possible to also study basolateral uptake and efflux of metabolites, nutrients and drugs.

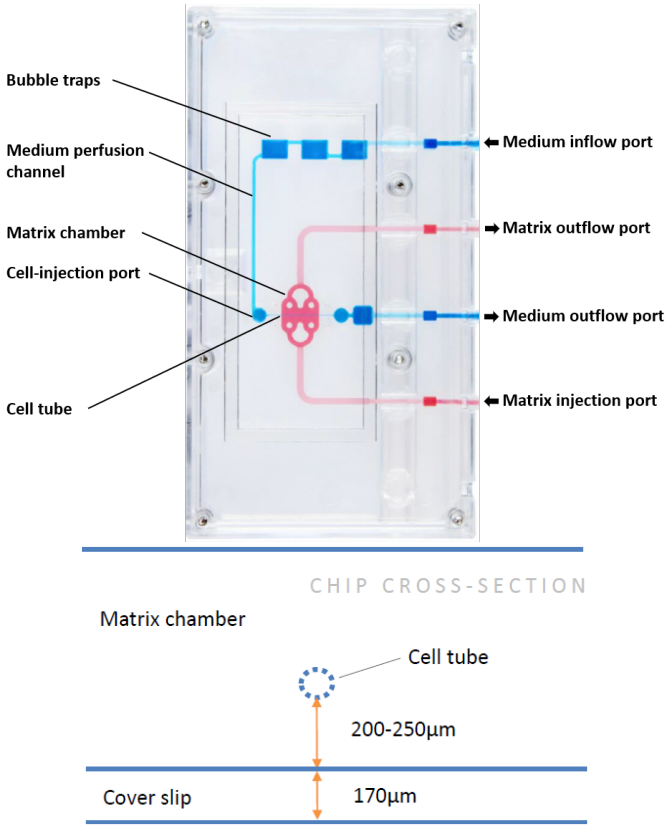

Figure 2.5: Schematic showing major components of Nortis ParVivo™ chips with cross-section showing the position of cell tube in the matrix chamber. (© Nortis, Inc., 2019)

Cells are introduced to the system via injection through the cell-injection port, and are cultured along the walls of the cell tube, forming a tubular 3D culture. HRPTEC cultured in the Nortis system have been shown to be polarized and to display formation of primary cilia in response to fluid shear stress.[8] Medium is perfused through the cell tube in a one-pass setup with no recirculation of medium. Medium flow through the chip is controlled by the Nortis ParVivo™ incubator gas pump and has been validated to produce a linear correlation between the wall fluid shear produced for flow rates between 0.8-2.5 µl/min, see Table 2.1.

Table 2.1: Specification of wall fluid shear stress generated and capacities at different flow rates in Nortis Parvivo™ chips.

Flow rate (µl/min)	Reservoir capacity (hours)	Wall shear stress (dyne/cm^2)
0.8	417	0.7
1	333	0.9
2	167	1.7
2.5	133	2.2

The wall fluid shear stress (τ_w) in the Nortis system is calculated using the Hagen-Poiseulle equation:[40]

$$\tau_w = \frac{4\mu Q}{\pi r^3} \tag{2.1}$$

Where μ is the dynamic viscosity of the culture medium ($1 * 10^{-4}$ Pa*s), r is the radius of the cell tube (62.5 µm) and Q is the volumetric flow rate. This gives an approximate value of the fluid shear experienced by HRPTEC exposed to flow in the Nortis system. For this thesis cells were cultured in the Nortis system at flow rates of 1 and 2 µl/min resulting in wall fluid shear stresses of 0.9 and 1.7 dyne/cm^2, see Table 2.1.

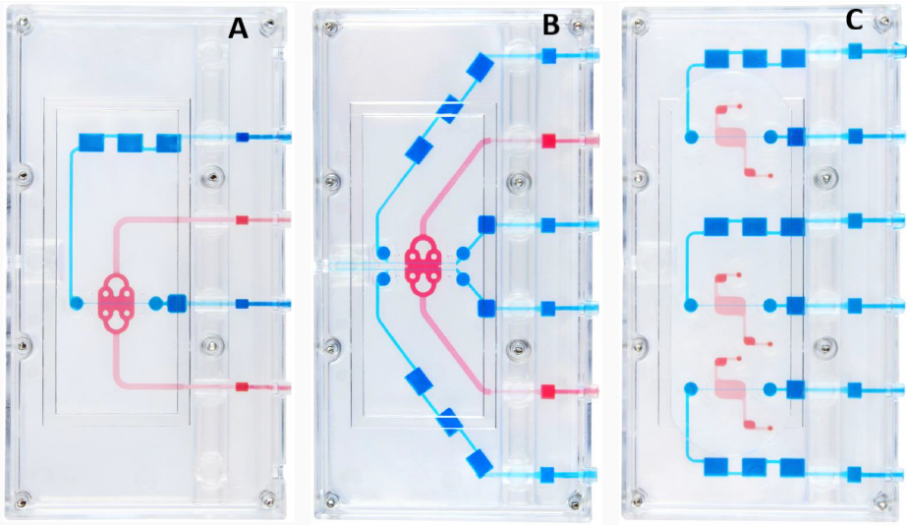

Figure 2.6: Three different types of Nortis ParVivo™ chips. Medium perfusion channels are marked in blue and matrix chamber and matrix injection channels are marked in red. **A**) Nortis ParVivo™ single channel chip. **B**) Nortis ParVivo™ dual channel chip. **C**) Nortis ParVivo™ triple channel chip. (© Nortis, Inc., 2019)

3. Materials & Methods

3.1 Materials

Cryopreserved primary human renal proximal tubule cells were purchased from Biopredic (Saint-Grégoire, France). Collagen I (rat tail) and Costar® multiple well cell culture plates were purchased from Corning (Corning NY, USA). Nortis ParVivo™ single, double and triple channel microfluidics chips, Nortis ParVivo™ incubator gas pump, Nortis ParVivo™ perfusion system, Nortis ParVivo™ perfusion platforms and associated inlet and outflow reservoirs were purchased from Nortis, Inc. (Seattle WA, USA). RLT lysis buffer and RNeasy Mini Kit were purchased from Qiagen (Hilden, Germany). Bovine serum albumin, FITC-labeled albumin (BSA-FITC), insulin-transferrin-sodium selenite media supplement (ITS), hydrocortisone (HC), epidermal growth factor (EGF), tri-iodothyronine (I3), fetal calf serum (FCS), dimethyl sulfoxide (DMSO), Triton™ X-100 and trypsin were purchased from Sigma Aldrich (Saint Louis MO, USA). Calcein-AM, PSC833, T25 and T75 culture flasks, MicroAmp™ optical 384-Well reaction plate, DMEM/F-12, GlutaMAX™ supplement basal medium, HBSS buffer, DPBS buffer, HEPES buffer, penicillin-streptomycin (10,000 U/mL), Hoechst 33342, Ethidium homodimer-1, ZO-1A12 mouse primary antibody, Goat anti-mouse Alexa Fluor 488 secondary antibody, CyQUANT™ LDH Cytotoxicity Assay, High-Capacity cDNA Reverse Transcription Kit with RNase Inhibitor, TaqMan™ Fast Advanced Master Mix and TaqMan™ Gene Expression Assay primer probes were purchased from Thermo Fisher Scientific (Waltham MA, USA).

Table 3.1: Media used in experiments and their supplements

Name	Base medium	Supplements
Basal medium	DMEM/F-12, GlutaMAX supplemented basal medium	None
Serum free medium	DMEM/F-12, GlutaMAX supplemented basal medium	EGF (10 ng/ml), HC (66 nM), I3 (5.9 pM), ITS (I: 10 µg/ml, T: 10µg/ml, S: 10 ng/ml)
Complete medium	DMEM/F-12, GlutaMAX supplemented basal medium	EGF (10 ng/ml), 1% FCS, HC (66 nM), I3 (5.9 pM), ITS (I: 10 µg/ml, T: 10µg/ml, S: 10 ng/ml)

3.2 Experimental overview

Chip experiments were conducted using the Nortis Parvivo™ system. HRPTEC were cultured in single or triple channel Nortis Parvivo™ chips (Figure 2.6A,C), with each channel considered as a technical replicate. First, the effects of long-term increased flow on chip cultured HRPTEC was evaluated. HRPTEC were exposed to two fluid shear stresses (0.9 and 1.7 dyne/cm^2) for a period of 5 weeks. This was then followed by comparison of differential gene expression and cytotoxicty in the two fluid shear stress conditions using qPCR and LDH activity assays, respectively. The LDH activity assay evaluates cytotoxicity by determining the release of the enzyme LDH into the cell culture medium. Since LDH can only be released into the medium if the membrane integrity of the cell is lost, measuring the LDH output provides a relative measurement of cytotoxicty in the chip cultures. These long-term flow studies served the purpose of determining if a 2-fold increase in fluid shear stress for 5 weeks, could be used to simulate a CKD-like response in the chip cultured HRPTEC.

Evaluation of cellular response to drug toxicity and endocytosis function was also investigated in the chip experiments. HRPTEC were cultured in the Nortis system at a fluid shear stress rate of 0.9 dyne/cm^2 for 1 week, followed by treatment with the antibiotic polymyxin B for 48 h at two different concentrations (50 or 150 µM) or fluorescein isothiocyanate labeled bovine serum albumin (BSA-FITC) (10 µg/ml). Toxicity induced by polymyxin B was evaluated using Live/Dead stains alongside LDH cytotoxicity assays. This was done to establish a positive control for drug toxicity and to establish if the HRPTEC used in this study display a similar sensitivity to polymyxin B as has been previously described in literature for HRPTEC cultures in the Nortis system.[35] The BSA-FITC fluorescence assay was performed to evaluate endocytosis as a complement to the Polymyxin B toxicity studies, as polymyxin B is taken up by HRPTEC by means of receptor mediated endocytosis.

Finally, cellular response to nutrient deprivation by clamping (halting medium flow completely) for 1, 3 or 7 days was evaluated in HRPTEC cultured in the Nortis system, with unclamped controls cultured at a fluid shear stress rate of 0.9 dyne/cm^2 for 1 week. Cell phenotype compared to unclamped control was then evaluated using qPCR and cell viability was assayed using Live/Dead stain. The purpose of these studies was to evaluate if nutrient deprivation and halting of flow could produce a stress response simulating ischemia in HRPTEC cultured in the Nortis system.

Experiments were also conducted on 2D cultured cells, exposing HRPTEC cultured on well plates to two orbital shear stresses (1.9, 5.3 dyne/cm^2) for 1 week with statically cultured cells as control. 2 or 3 wells were used to evaluate each condition with the mean of the wells considered as a biological replicate. Differential gene expression between flow exposed and static cell cultures was evaluated using qPCR, alongside evaluation of drug transport function by P-gp mediated efflux, and endocytosis using Calcein-AM and BSA-FITC fluorescence assays, respectively. This was done to evaluate changes to cell phenotype in response to orbital flow exposure in 2D and to establish if the HRPTEC used in this study display similar functional changes in response to flow to what has been previously described in literature.[31,11] Differential gene expression between 3D cultured HRPTEC (0.9 dyne/cm^2, 1 and 5 week culture) and 2D cultured HRPTEC (static, 1 week culture) was then evaluated by comparing qPCR data from previous 2D and 3D experiments. These experiments were conducted to establish if a difference in HRPTEC

phenotype by gene expression could be detected when transitioning from 2D well plate cultures to 3D chip cultures.

3.3 HRPTEC culture

Commercially obtained cryopreserved primary HRPTEC, passage 2, ($1 * 10^6$ cells/vial) derived from healthy tissue extracted from kidney resections, were cultured to form a tubular cell layer in the Nortis ParVivo™ chips. For the 1.7 dyne/cm^2 pilot experiment the cells were started in a T75 culture flask, for all other experiments cells were started in T25 culture flasks. Cells were thawed in a 37 °C water bath and immediately transferred to complete medium, see Table 3.1. The cell suspension was centrifuged at 300 x g, 4 °C for 5 minutes, the supernatant was aspirated and the cells were resuspended in 5 or 11 ml (T25 or T75) of complete medium. The cells were seeded in T25 or T75 culture flasks and incubated at 37 °C, 5% CO_2 for 3 days before harvest. Prior to harvest, medium was aspirated from the culture flasks and cells were washed with HBSS (T25: 3 to 5 ml, T75: 8 to 10 ml) to remove any residual medium and dead cells. 1 or 2 ml of trypsin (T25 or T75) was used to detach cells from culture flask surface, and cells were treated with trypsin for 2-2.5 minutes at 37 °C. Cell detachment was then confirmed with phase contrast microscopy and complete medium was added (T25: 5 ml, T75: 11 ml) to dilute and inactivate the trypsin and resuspend the cells. Cell suspension was then centrifuged at 300 x g, 22 °C for 5 minutes. 0.5 ml of cell suspension was reserved for cell count and viability assessment. Supernatant was aspirated and cell pellet was resuspended in complete medium.

For the chip-based experiments cells, were diluted to a concentration between $1 * 10^6$ cells/100 µl and $2 * 10^6$ cells/100 µl for all experiments. Cell count and viability was determined using a NucleoCounter® NC-200™ (ChemoMetec, Lillerød, Denmark).

For 2D experiments, cells were diluted to a concentration of 75 000 cells/cm^2 and seeded in 12 well plates. All well plates were incubated at 37 °C, 5% CO_2 for 24 hours to allow cells to attach to the wells. After 24 hours, plates designated for flow treatment were transferred to a VWR™ microplate shaker (VWR International, USA). The distribution of fluid shear stress in the wells can be seen in Figure 3.1 and the maximum fluid shear stress experienced by the cells ($\tau_{o,max}$) was calculated using the following equation.[41]

$$\tau_{o,max} = a\sqrt{\rho\mu(2\pi f^3)} \tag{3.1}$$

In this equation, a is the radius of rotation of the orbital shaker (3 mm), ρ is the density of the cell culture medium (1 g/ml), μ is the dynamic viscosity of the cell culture medium ($1 * 10^{-4}$ Pa*s) and f is the frequency of the orbital shaker. Two shaking frequencies were chosen for the two flow conditions 150 ($\tau_{o,max}$ = 1.9 dyne/cm^2) or 300 rpm ($\tau_{o,max}$ = 5.3 dyne/cm^2) in the incubator, while control plates were left static. The cells were matured for 6 days on complete medium before transporter activity evaluation and gene expression assays were performed. Medium was refreshed every 2-3 days.

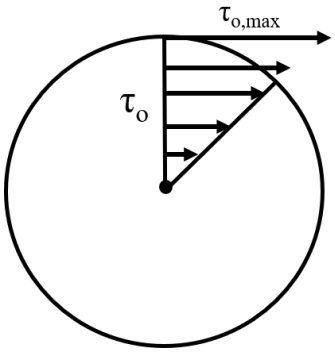

Figure 3.1: Schematic of shear stress (τ_o) distribution in 2D well plate cultures exposed to orbital flow, with the maximum orbital shear stress indicated as $\tau_{o,max}$.

3.4 Chip experiments

3.4.1 Chip preparation

Nortis ParVivo™ chips were prepared by first washing the matrix chambers with 2 to 3 ml 99.8% ethanol to remove PBS from the chamber. The ethanol was then aspirated for 2-3 minutes until the chamber was dry. Next, Nortis ParVivo™ chips were injected with a premixed collagen I solution containing a final concentration of DPBS (10%), phenol red (0.04 mg/ml), HEPES (25 mM), genipin (0.2 mM) NaOH (to pH 8-8.5) and collagen I (7 mg/ml). The chips were transferred to (4 °C) for a minimum of 1 hour, then incubated (37 °C) overnight, to allow polymerization. Following overnight incubation, the fiberglass pin was removed, creating a cylindrical channel (125 µm in diameter) in the collagen matrix. The chips were then perfused with complete medium overnight to ensure that the channel was filled with medium. Prior to cell seeding the channel was coated with collagen IV (0.3 mg/ml) to improve cell adhesion, by injecting 2x 2.5 µl, followed by incubation at 37 °C. Cells were then injected (1x 2.5 µl) into the channel at $1 * 10^6$ - $2 * 10^6$ cells/100 µl. Cell density in the channel was evaluated with phase contrast microscopy to determine if an additional cell injection was needed. Next, the chips were incubated static overnight to allow cell attachment. To allow for cell maturation, all chips were first perfused with complete medium at 1 µl/min, yielding a fluid shear stress of 0.9 dyne/cm^2. 4 days after cell injection, medium was replaced with serum free medium (SFM).

3.4.2 Cytotoxicity and gene expression analysis with long-term increased flow exposure

For the chip-based increased flow experiments, perfusion rate was increased from 1 to 2 µl/min and switched to serum free medium on the fifth day of culture, yielding a fluid shear stress of 1.7 dyne/cm^2. Increased flow was sustained for an additional 4 weeks, while perfusion of control chips remained at 1 µl/min. Every 7 days, 24 hour perfusion samples were taken to evaluate perfusion rate. Lactate dehydrogenase (LDH) activity was determined on perfusate samples using CyQUANT™ LDH Cytotoxicity Assay according to manufacturer's instructions to evaluate viability over time. Statistical analysis was performed in GraphPad Prism 8.0.1 (GraphPad Software, San Diego, CA, USA). Difference

between treatment and control was tested at each time point with two way ANOVA with Sidak's correction for multiple comparisons and was defined as statistically significant at $p < 0.05$. After 5 weeks of culture, chips were connected to a syringe pump, enabling non-sterile work, and washed with HBSS at 1 µl/min for 2 hours. To lyse the cells, the chips were perfused with RLT lysis buffer for 20 minutes at 5 µl/min. The chips were then incubated at room temperature for 30 min, before perfusion was started again for 30 min at 5 µl/min. Outflow from chips during RLT perfusion was collected as sample.

3.4.3 Polymyxin B sensitivity and endocytosis activity with short-term increased flow exposure

In the chip-based endocytosis experiments, chips were treated with the nephrotoxic antibiotic polymyxin B or fluorescently labeled (FITC) BSA after 1 week of culture, to evaluate drug sensitivity and endocytosis in HRPTEC grown in the Nortis ParVivo™ system exposed to regular flow (1 µl/min) or increased flow (2 µl/min).

Polymyxin B was used to evaluate drug induced toxicity in chip cultured HRPTEC. After one week of culture, cells were exposed to polymyxin B (50 or 150 µM) or vehicle (MQ) for 48 h in SFM at a flow rate of 1 µl/min. 24 h perfusion samples were taken before and 24 and 48 h after exposure. After 48 h, Live/Dead stain was performed to evaluate endpoint cell count and viability. To this end, chips were perfused with HBSS containing Hoechst 33342 (10 µg/ml) and ethidium homodimer-1 (2 µM) at 1 µl/min for 2 hours. Live/Dead stain fluorescence was evaluated using ImageXpress®Micro Confocal microscope (Molecular Devices, San Jose, CA, USA). Image processing and cell count (Noise tolerance [NT]: 1000-6000) was performed in ImageJ 1.52a. Cell count based viability was calculated using the formula: *(Total cell count - Dead cell count) / Total cell count.* Graphs were plotted in GraphPad Prism.

ZO-1 immunofluorescence stain was performed to evaluate tight junctions following polymyxin B treatment. Cells were fixed and permeabilized by perfusion with 4% paraformaldehyde (PFA) at 3 µl/min for 45 min then washed, blocked and permeabilized by perfusion with wash solution, BSA (2%) and Triton™ X-100 (0.5%) in HBSS, at 10 µl/min for 45 min. Cell channels were then injected with 200 µl ZO1-1A12 mouse primary antibody in wash solution (1:50, Invitrogen) and incubated at 4°C overnight. Chips were then perfused with goat anti-mouse secondary antibody (Alexa Fluor 488, 1:100, Life Technologies) in wash solution at 10 µl/min for 45 min, making sure to protect chips from light. Prior to imaging, the chips were washed with wash solution at 10 µl/min for 45 min to remove any remaining unbound secondary antibody from the channels. Immunofluorescence signal was imaged using ImageXpress®Micro Confocal microscope (Molecular Devices, San Jose, CA, USA). Image processing was performed in ImageJ.

To evaluate cytotoxicity upon polymyxin B treatment, lactate dehydrogenase (LDH) was determined in perfusion samples using the CyQUANT™ LDH Cytotoxicity Assay according to manufacturer's instructions. Statistical analysis was performed in GraphPad Prism. Difference between treatment and control was tested at each time point with two way ANOVA using Sidak's correction for multiple comparisons and was defined as statistically significant at $p < 0.05$.

Endocytosis activity was also evaluated in the Nortis chips using BSA-FITC. Cells were exposed apically to BSA-FITC (10 µg/ml) with and without BSA (10 mg/ml) for inhibi-

tion, in SFM for 24 h at a perfusion rate of 1 µl/min. Before imaging, cells were washed with HBSS containing Hoechst 1:1000 v/v for 2.5 h. Fluorescence signal was imaged using ImageXpress® Micro Confocal microscope. Image processing was performed in ImageJ.

3.4.4 Clamping experiments

Clamping experiments were performed to evaluate the effects of nutrient deprivation and the absence of flow on HRPTEC cultured in the Nortis system, as would be seen in ischemia or *in vivo* clamping experiments. Medium perfusion (1 µl/min) was stopped for 1, 3 or 7 days, as seen in clamping scheme in figure 3.2. Live/Dead stain was performed after clamping as described for the polymyxin B experiment above. To evaluate endpoint gene expression after clamping, chips were connected to a syringe pump and washed with HBSS at 1 µl/min for 2 hours. To lyse the cells, the chips were perfused with RLT lysis buffer for 20 minutes at 5 µl/min. The chips were then incubated at room temperature for 30 min before perfusion was started again for 30 min at 5 µl/min. Outflow from chips during RLT perfusion was collected as sample.

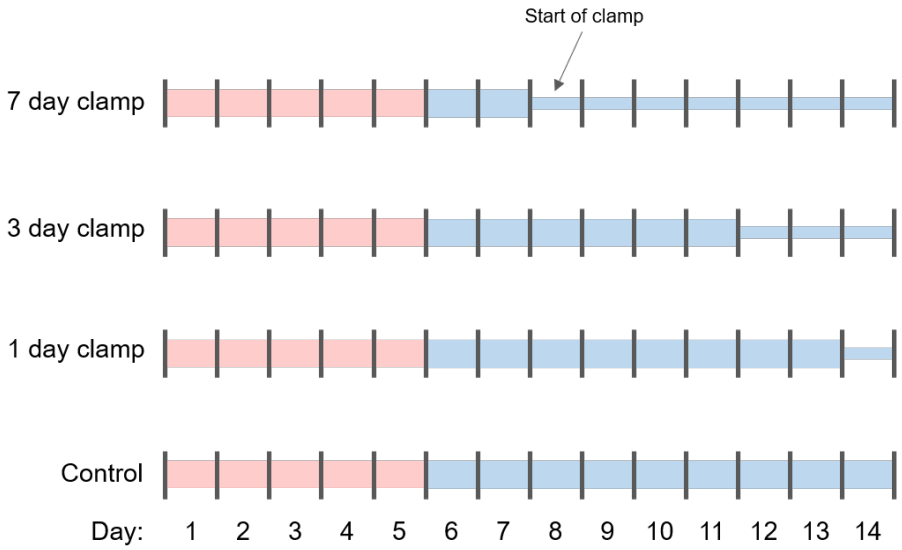

Figure 3.2: Timeline schematic of clamping experiments performed on HRPTEC in Nortis Parvivo™ triple channel chips. Pink segments represent culture on complete medium, blue segments represent culture on serum free medium, thick segments represents unclamped culture duration and thin segments represent clamped culture duration.

3.5 2D orbital shaker experiments

3.5.1 RNA harvest & transporter activity

RNA was harvested by first washing cells 3 times with 1 ml HBSS, cells were then lysed with 1 ml RLT lysis buffer per well. RLT lysis buffer was collected as sample. To evaluate the effect of fluid shear stress on the transport activity of the efflux transport protein P-gp, the fluorescent substrate calcein was used. Calcein-AM diffuses freely into the

cell and is metabolised upon cellular uptake into the fluorescent compound calcein, a substrate for P-gp. Specificity of the substrate was confirmed using the P-gp inhibitor PSC833. Before treatment, medium was aspirated and cells were washed 3 times with HEPES (10 mM) in HBSS. Cells were exposed to calcein-AM (1 µM) with or without PSC833 (5 µM) or only HEPES (10 mM) in HBSS, for 1 hour at 37°C to allow calcein accumulation. Next, wells were washed three times with 1 ml cold (4°C) HEPES (10 mM) in HBSS before lysation with 0.5 ml 1% Trition in HBSS solution at 4°C. Wells were then incubated for 1 hour at 37°C. Fluorescence was measured (wavelengths: excitation 485 nm; emission 535 nm) using a Clariostar plate reader (BMG Labtech, Germany). Data was analysed using GraphPad Prism and blank-subtracted. Statistical analysis was performed in GraphPad Prism. Difference between treatment and control was tested with a paired t-test and was defined as statistically significant at $p < 0.05$. BSA-FITC assay was used to evaluate the effect of flow on endocytosis activity in 2D. 24 hours before treatment, cells were washed three times with SFM and switched from complete to SFM, to starve cells of serum and increase sensitivity of the assay. On the day of the assay, cells were washed 3 times with serum free medium and exposed to BSA-FITC (50 µg/ml) with or without BSA (10 mg/ml) for inhibition in SFM, and incubated (37 °C) for 2 h. Cells were harvested using trypsin (200 µl/ well), resuspended in complete medium (800 µl/well) and samples were transferred to Eppendorf tubes. After centrifugation (1000 rpm, 5 min, 4 °C), supernatant was removed and the pellet was resuspended in HBSS. Following another centrifugation, cells were resuspended in PFA (0.5%) for fixation. Fluorescence was evaluated by flow cytometry in BD LSR-Fortessa™ (BD Biosciences, Franklin Lakes, NJ, USA) using channel FITC-A. Data was analysed by calculating the geometric mean of the FITC histogram for each sample using FlowJo (FlowJo, LLC, Ashland, OR, USA) and graphs were plotted in Graphpad Prism.

3.6 Gene expression assays

RNA was isolated from 2D and 3D lysis samples using RNeasy Mini Kit according to the manufacturer's instructions. RNA concentration was measured using Nanodrop microvolume spectrophotometer (Saveen Werner AB, Sweden). cDNA was synthesized from RNA samples using High-Capacity cDNA Reverse Transcription Kit with RNase Inhibitor, according to the manufacturer's instructions, in an Eppendorf 5333 Mastercycler (Eppendorf AG, Germany). cDNA samples were diluted and qPCR assay was performed with Taqman™ primer probes in a QuantStudio™ 7 Flex Real-Time PCR System (Thermo Fisher Scientific, USA). For a complete list of genes evaluated see Table 3.2. Ct values from qPCR analysis were exported to GraphPad Prism 8.0.1 and normalized against static control, using *GAPDH* as reference gene, to generate -ΔΔCt values. Statistical analysis was performed in GraphPad Prism on -ΔΔCt values using separate t-tests for each gene, using the Holm-Sidak method to correct for multiple comparisons. Difference between flow and static was defined as statistically significant at $p < 0.05$, indicated as *.

Table 3.2: Genes screened in qPCR assays, their associated proteins as well as indication of function associated with gene expression.

Gene name	Protein	Indication
Kidney injury markers:		
COL1A1	Collagen I	Matrix deposition, Fibrosis
COL1A2	Collagen I	Matrix deposition, Fibrosis
TGFB1	TGF-β	Kidney damage, Fibrosis
IL6	IL6	Kidney damage
HAVCR1	KIM-1	Proximal tubule damage
Transport proteins & endocytosis receptors:		
ABCB1	P-gp	Efflux transport
ABCC4	MRP4	Efflux transport
SLC22A2	OCT2	Uptake transport*
SLC22A6	OAT1	Uptake transport
SLC22A8	OAT3	Uptake transport
SLC47A1	MATE-1	Efflux transport*
SLC47A2	MATE2-K	Efflux transport*
SLC5A2	SGLT2	Glucose transport
CUBN	Cubilin	Receptor mediated endocytosis
LRP2	Megalin	Receptor mediated endocytosis
Oxidative stress & hypoxia markers:		
HMOX1	HO-1	Oxidative stress
HIF1A	HIF1-α	Oxidative stress
Proximal tubule & epithelial markers:		
AQP1	Aquaporin-1	Water transport
TJP1	Tight junction protein 1	Tight junction formation
GGT1	Glutathione hydrolase 1 proenzyme	Proximal tubule marker
Reference genes:		
GAPDH	Glyceraldehyde-3-phosphate dehydrogenase	Reference
HPRT1	Parafibromin	Reference

*Function in the proximal tubule

4. Results

4.1 Effect of flow on gene expression and transport activity in 2D HRPTEC cultures

To evaluate the effect of fluid shear stress on 2D HRPTEC cultures, cells were cultured in 12 well plates and exposed to a maximum orbital shear stress of 1.9 or 5.3 dyne/cm^2 along with a static control for one week. Phenotype was analysed through gene expression of drug transporters and proximal tubule and cell stress markers. Results from qPCR analysis of 2D flow experiments are presented in Figure 4.1. Differential gene expression of more than 2-fold (-ΔΔCt <-1 and >1) was arbitrarily considered physiologically relevant.

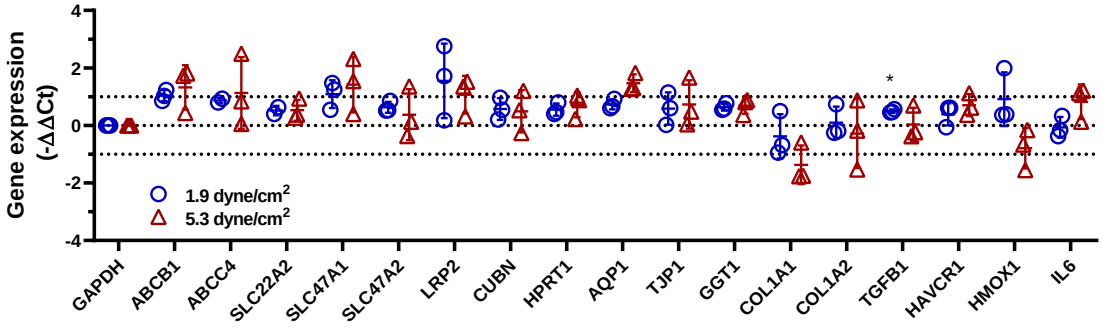

Figure 4.1: Differential gene expression in 2D cultured HRPTEC exposed to a fluid shear stress of 1.9 dyne/cm^2 or 5.3 dyne/cm^2 compared to static control. Data is presented as mean ± SD of three separate experiments analysed in triplicate (n=3). Dotted lines represent cut-off value relevance of differential gene expression (-ΔΔCt <-1 and >1). Expression at 1.9 or 5.3 dyne/cm^2 was normalized against static control using GAPDH as reference gene to generate -ΔΔCt values. Statistical analysis was performed using separate t-tests, one per gene, Holm-Sidak method was used to correct for multiple comparisons (*p $<$ 0.05).

The only significant change to gene expression detected in this assay was upregulation of TGF-β in cells exposed to a shear stress rate of 1.9 dyne/cm^2. The upregulation is however below the cut-off value (-ΔΔCt $<$ 1) with no significant change to gene expression in other markers for this condition. Reproducibilty was low for this analysis and large variations in gene expression can be clearly seen between experiments in both conditions. Two out of three experiments in the 5.3 dyne/cm^2 condition produced similar results (Figure 4.1), with a general trend towards increased expression of transporter, endocytosis and proximal tubule marker genes, most notably *LRP2* and *SLC47A1*. One experiment conducted for this condition produced contradictory results, showing almost no change to gene expression compared to static control. It could not be concluded that this was the result experimental error, as the same procedure was used for each experiment, suggesting that further study is needed to determine if HRPTEC maintain a stable phenotype during orbital flow treatment.

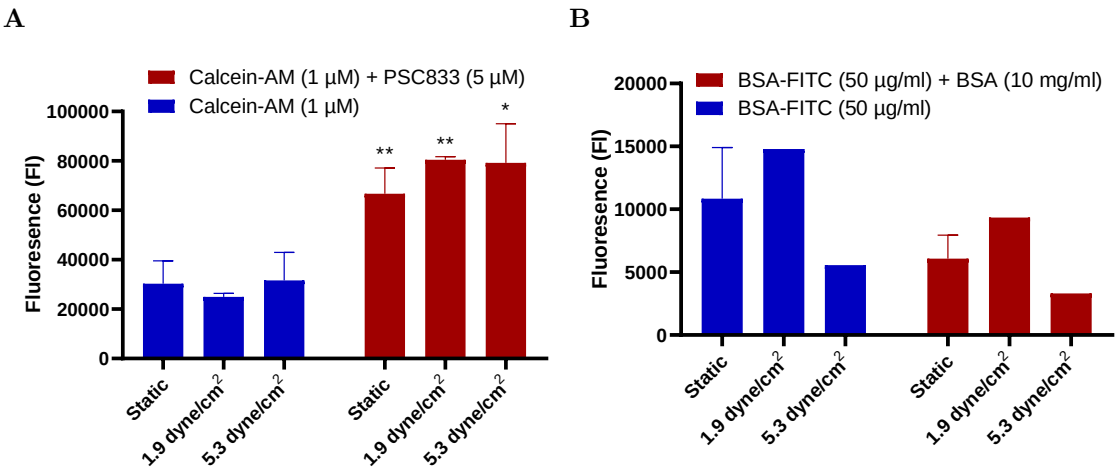

Figure 4.2: 2D fluorescence assays. **A.** Fluorescence results from 2D calcein-AM assay. Data was blank-subtracted and is presented as mean ± SD of three separate experiments performed in triplicate (n=3). Statistical analysis was performed using separate t-tests, one per condition, Holm-Sidak method was used to correct for multiple comparisons (*p $<$ 0.05, **p $<$ 0.01). **B.** Fluorescence results from 2D BSA-FITC assay. Data was blank-subtracted and is presented as mean ± SD of one experiment performed in triplicate (n=1).

To evaluate the effect of flow on P-gp activity of HRPTEC grown in 2D cultures, cells were exposed to fluid shear stress rates of 1.9 dyne/cm^2 or 5.3 dyne/cm^2 and compared to static controls. Cells were exposed to flow for 1 week before treatment with Calcein-AM and P-gp inhibitor PSC833. Fluorescence results of calcein-AM assay are presented in Figure 4.2A. Inhibition of calcein efflux was successful, with a significant increase in fluorescence signal seen in all conditions when comparing inhibited to uninhibited samples. However, no significant difference in calcein efflux could be detected in HRPTEC exposed to flow compared to static control. This indicates that function of P-gp is present in HRPTEC used in the experiment but that no regulation of this function can be detected as a result of flow and increased fluid shear stress. Endocytosis was then evaluated using the same culture protocol as above. Cells were exposed to flow for 1 week before treatment with BSA-FITC and inhibitor BSA. Fluorescence results of BSA-FITC are presented in Figure 4.2B. BSA-FITC uptake and inhibition by non-labelled BSA was detected in all conditions, indicating that endocytic function is present in 2D cultured HRPTEC. BSA-FITC uptake does not seem to be affected by flow in HRPTEC exposed to flow compared to static control, and the lack of biological replicates (n=1) does not allow statistical analysis. In addition, large variations in uptake can be seen for the static control, suggesting the method used was too unspecific to accurately evaluate endocytic uptake.

4.2 Chip-based experiments

4.2.1 Effect of flow on cytotoxicity and gene expression in chip cultured HRPTEC

To evaluate how fluid shear stress affects HRPTEC in long-term culture, cells were cultured in the Nortis system for 5 days at 0.9 dyne/cm^2 in complete medium. Next, cultures were exposed to a fluid shear stress of 0.9 or 1.7 dyne/cm^2, switched to SFM, and HRPTEC were cultured for another 4 weeks.

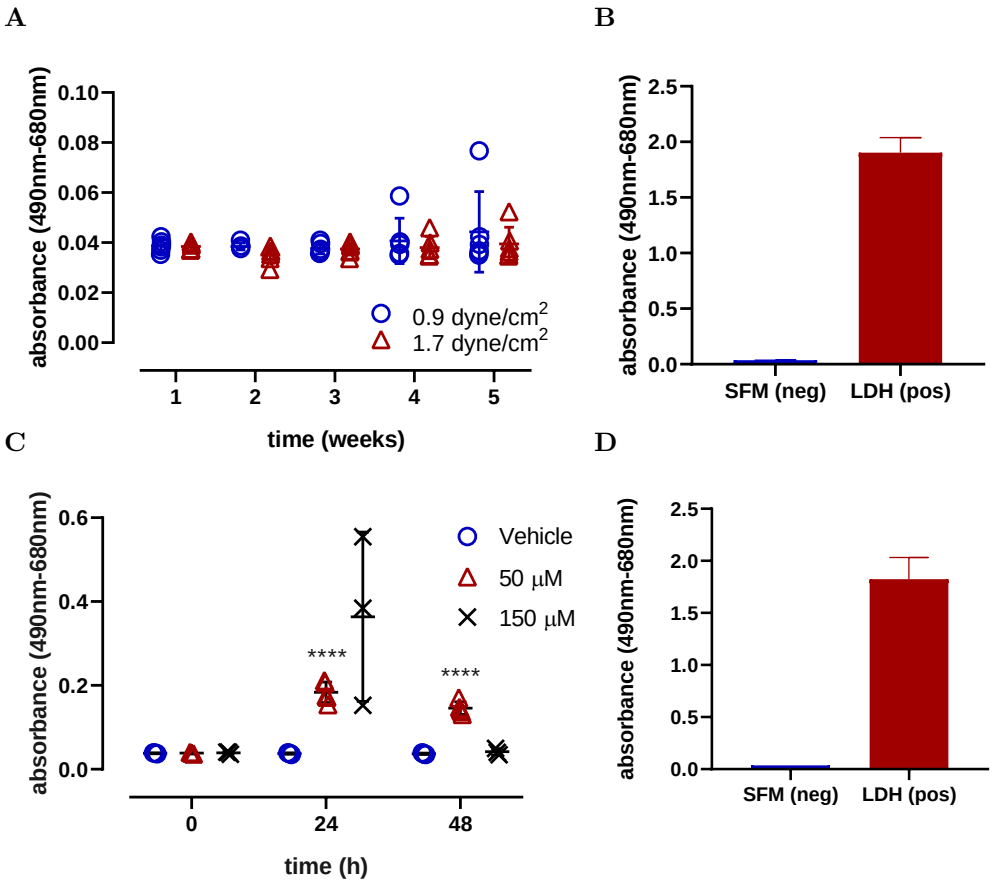

Figure 4.3: LDH activity in 3D cultured HRPTEC treated with increased flow or polymyxin B . **A.** Absorbance data from LDH activity assay of HRPTEC exposed to a fluid shear stress of 0.9 or 1.7 dyne/cm^2. Data is presented as mean ± SD of six separate experiments (n=6). Statistical analysis was performed using 2-way ANOVA, Sidak method was used to correct for multiple comparisons. **B.** Assay controls (negative: SFM, positive: max assay activity) for LDH activity assay of increased flow treated HRPTEC (n=2). **C.** Absorbance data from LDH activity assay of polymyxin B (50, 150 µM; 48 h) treated HRPTEC, data is presented as mean ± SD of three (150 µM), four (vehicle), or five (50 µM) separate experiments (n=3, n=4, n=5). Statistical analysis was performed using 2-way ANOVA, Sidak method was used to correct for multiple comparisons (****$p < 0.0001$). **D.** Assay controls (negative: SFM, positive: max assay activity) for LDH activity assay of polymyxin B treated HRPTEC (n=2).

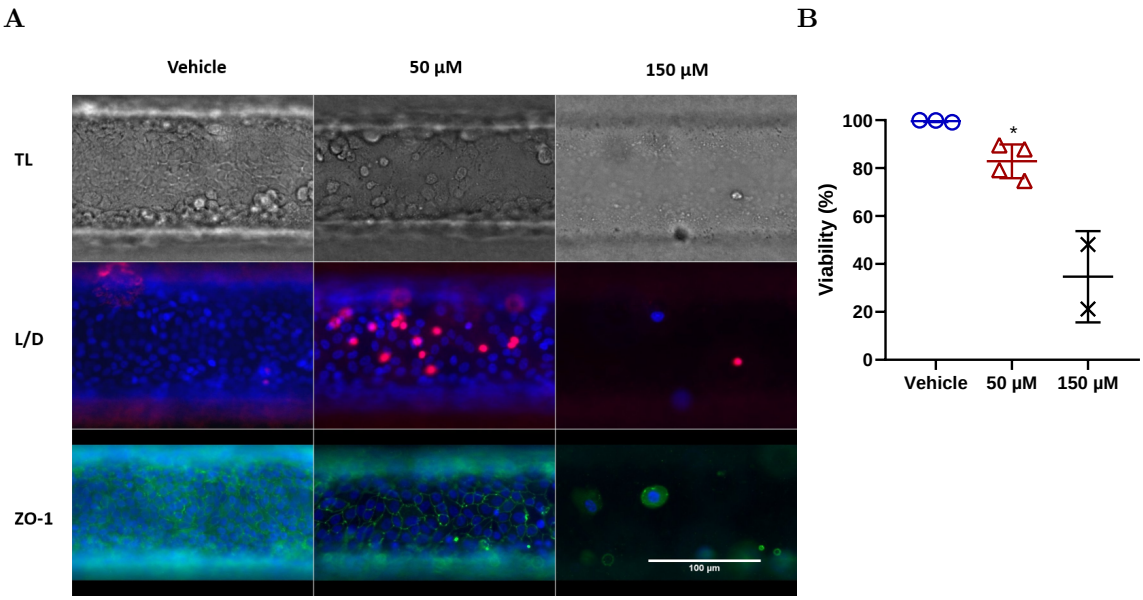

Figure 4.4: Viability and immunofluorescence assays in 3D cultured HRPTEC treated with Polymyxin B. Data from Live/Dead stain of polymyxin B (50, 150 µM; 48 h) treated HRPTEC, is presented as representative images or mean ± SD of two (150 µM), three (vehicle) or four (50 µM) separate experiments (n=2, n=3, n=4). Data from ZO-1 immunofluorescence stain is presented as representative images of one experiment (n=1). **A.** Representative transmitted light (TL), Live/Dead (L/D) stain and ZO-1 immunofluorescence stain images of 3D cultured HRPTEC. In the L/D stain, cell nuclei are shown in blue with dead cell nuclei shown in red. In the ZO-1 stain cell nuclei are shown in blue with tight junction proteins in green. **B.** Endpoint (48h) cell count based viability assay based on Live/Dead stain. Statistical analysis was performed using a student's t-test for each condition, (*$p < 0.05$)

Lactate dehydrogenase activity (LDH) activity of the perfusate samples remained stable and close to ($\sim$ 0.04) to negative control ($\sim$ 0.04) (Figure 4.3A,B) throughout the entire culture period, suggesting that viability was maintained in chip cultured HRPTEC for up to 5 weeks in SFM. Outliers can be seen for cells exposed to a fluid shear stress of 0.9 dyne/cm^2 at 4 and 5 weeks, however, absorbance values remained relatively low (0.059-0.072) with both outliers being contained within a single experiment. To evaluate endocytic function and establish a positive control for LDH activity as a measure of toxicity in chip cultured HRPTEC, cells were cultured in complete medium for one week, followed by SFM for an additional week. HRPTEC were then exposed to the nephrotoxicant polymyxin B at 50 or 150 µM for 48 h. LDH activity in the perfusate significantly demonstrates cytotoxicity when exposed to 50 uM for both 24 and 48 h (Figure 4.3C). A near 5-fold difference to LDH activity can be seen when comparing cells treated with 50 µM polymyxin B for 24 h (0.184 ± 0.024, Figure 4.3C) to cells exposed to a fluid shear stress of 0.9 (0.044 ± 0.016) or 1.7 (0.039 ± 0.007) dyne/cm^2 for 5 weeks (Figure 4.3A). This further supports the abscence of cell toxicity in long-term HRPTEC cultures. For the 150 µM condition, no significant results indicating toxicity could be obtained, while an increase in LDH activity can be seen after 24 h of treatment (Figure 4.3A). Exposure to 150 uM increased LDH in the supernatant at 24 h (Figure 4.3B) and reduced viability as evaluated by Live/Dead stain (34.7 ± 19.1%, Figure 4.4B), but were not significant due to

high variation. This is explained by HRPTEC being washed out of the chip (Figure4.4A), indicating profound toxicity induction.

Polymyxin B (50 µM, 48 h) significantly reduced the viability of HRPTEC cultured in Nortis chips to 83 ± 7.0% compared to vehicle (Figure 4.4B). This is the result of an increase in ethidium positive cells and a reduction of total cell count, and is supported by morphological changes seen in Figure 4.4A. ZO-1 immunofluorescense stain also showed that the cell density and total tight junction staining are reduced (Figure 4.3A), suggesting cells cover a larger surface area, in order to maintain integrity of the epithelial layer. These results indicate that HRPTEC cultured in Nortis chips are sensitive to polymyxin B, suggesting that endocytosis function is active.

It is now established that HRPTEC remain viable in the the Nortis system for up to 5 weeks, however, this system was also employed to evaluate the long-term effects of flow on HRPTEC phenotype. Therefore, differential gene expression of several drug transporters, proximal tubule and cell stress markers in HRPTEC exposed to regular flow (1 µl/min) were compared to HRPTEC exposed to a 2-fold increase (2 µl/min) to flow rate, corresponding to a fluid shear stress of 0.9 and 1.7 dyne/cm^2, respectively. Results from qPCR analysis of 5 week increased fluid shears stress cultures are shown in Figure 4.5. Gene expression was not significantly different when fluid shear stress was increased from 0.9 to 1.7 dyne/cm^2 suggesting that these phenotypic markers are not affected by flow. Surprisingly, regained expression of *SLC22A6* and *SLC22A8* was detected in both fluid shear stress conditions. Expression of drug transporter genes *SLC22A6* and *SLC22A8* could only be detected in chip cultured cells, *SLC22A6* in both 1 and 5 week cultures and *SLC22A8* only in 5 week cultures. This indicates an improved proximal tubule phenotype in the chip cultured HRPTEC as a result of long term (5 weeks) culture in SFM. It should however be mentioned that expression of *SLC22A8* was close to the limit of detection for the qPCR assay, suggesting a very low level of expression.

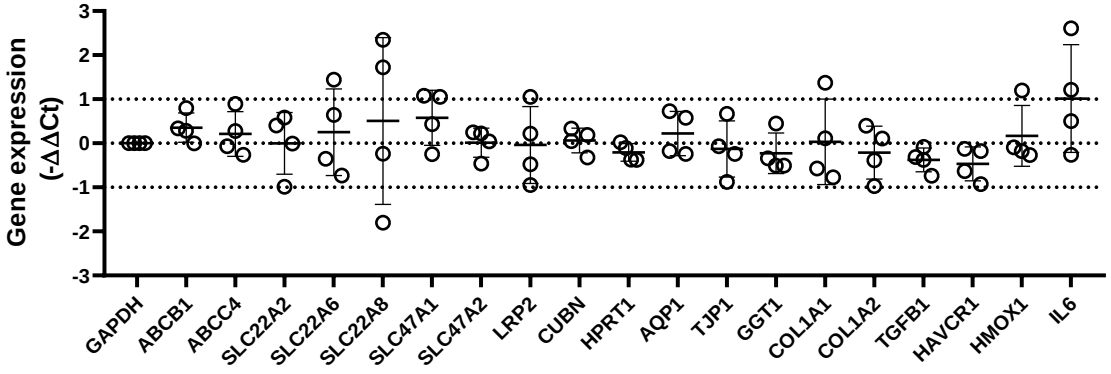

Figure 4.5: Differential gene expression in 3D cultured HRPTEC exposed to an increased fluid shear stress of 1.7 dyne/cm^2 compared to 0.9 dyne/cm^2. Data is presented as mean ± SD of four separate experiments performed in triplicate (n=4). Dotted lines represent cut-off value for relevance of differential gene expression (-ΔΔCt <-1 and >1). Expression at 1.7 dyne/cm^2 was normalized against 0.9 dyne/cm^2, using GAPDH as reference gene to generate -ΔΔCt values. Statistical analysis was performed using separate t-tests, one per gene, Holm-Sidak method was used to correct for multiple comparisons.

4.2.2 Effects of chip culture on gene expression in HRPTEC

To evaluate cell phenotype of chip cultured (0.9 dyne/cm^2) HRPTEC compared to 2D cultured HRPTEC, gene expression of 3D SFM HRPTEC cultures (1, 5 weeks) were compared to 1 week static 2D cultures in complete medium. Upregulation of drug transporter genes *SLC47A1* (41.3 ± 3.4 fold, 33.2 ± 13.2 fold), *SLC47A2* (71.9 ± 8.9 fold, 99.6 ± 61.7 fold) and *LRP2* (46.7 ± 13.1 fold, 67.5 ± 34.1 fold) could be seen in both 1 and 5 week 3D cultures, with additional upregulation of *SLC22A2* (3.6 ± 1.1 fold) only for the 5 week cultures (Figure 4.6). This suggests an improved phenotype in terms of drug transport capability in chip cultured cells compared to 2D cultured cells. Downregulation of stress markers *COL1A1* and *HMOX1* was also seen in long and short term 3D cultures, as well a significant decrease in *HAVCR1* expression in short term cultures. Expression of all other evaluated stress markers (Table 3.2) is not significantly different when comparing 1 and 5 week chip cultures. This suggests that cell phenotype remains stable over time in chip cultured HRPTEC and that a proximal tubule phenotype more suitable for drug transport or toxicity studies, in both long and short term, is achieved in HRPTEC cultured in the Nortis system compared to 2D cultures.

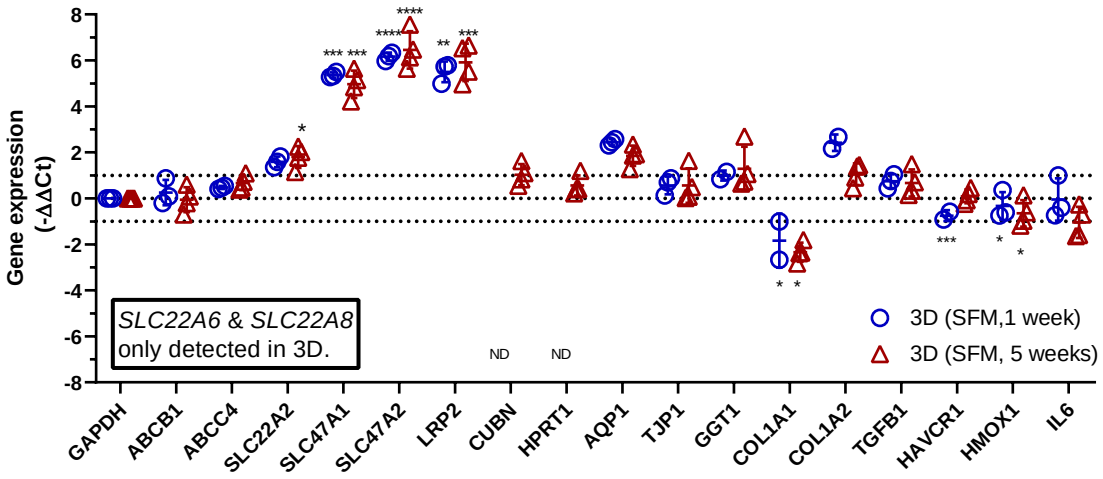

Figure 4.6: Differential gene expression in 3D cultured HRPTEC compared to static 2D cultures. 1 and 5 week 3D HRPTEC cultures exposed to a fluid shear stress of 0.9 dyne/cm^2 compared to 2D static control. Data is presented as mean ± SD of three (1 week) or four (5 week) separate experiments analysed in triplicate (n=3, n=4). Dotted lines represent cut-off value for relevance of differential gene expression (-ΔΔCt <-1 and >1). Data was normalized against static 2d cultures using *GAPDH* as a reference gene to generate -ΔΔCt values. Statistical analysis was performed using separate t-tests, one per gene, Holm-Sidak method was used to correct for multiple comparisons (*p < 0.05, **p < 0.01, ***p < 0.001, ****p < 0.0001). Genes not evaluated for specific conditions are marked with ND for not determined.

4.2.3 Effect of nutrient and flow deprivation on chip-cultured HRPTEC

To evaluate the effects of nutrient and flow deprivation on viability and differential gene expression in HRPTEC cultured in the Nortis system cells were cultured for 1 week on complete medium, before being switched to serum free medium and clamped, resulting in a complete absence of medium flow for 1, 3 or 7 days.

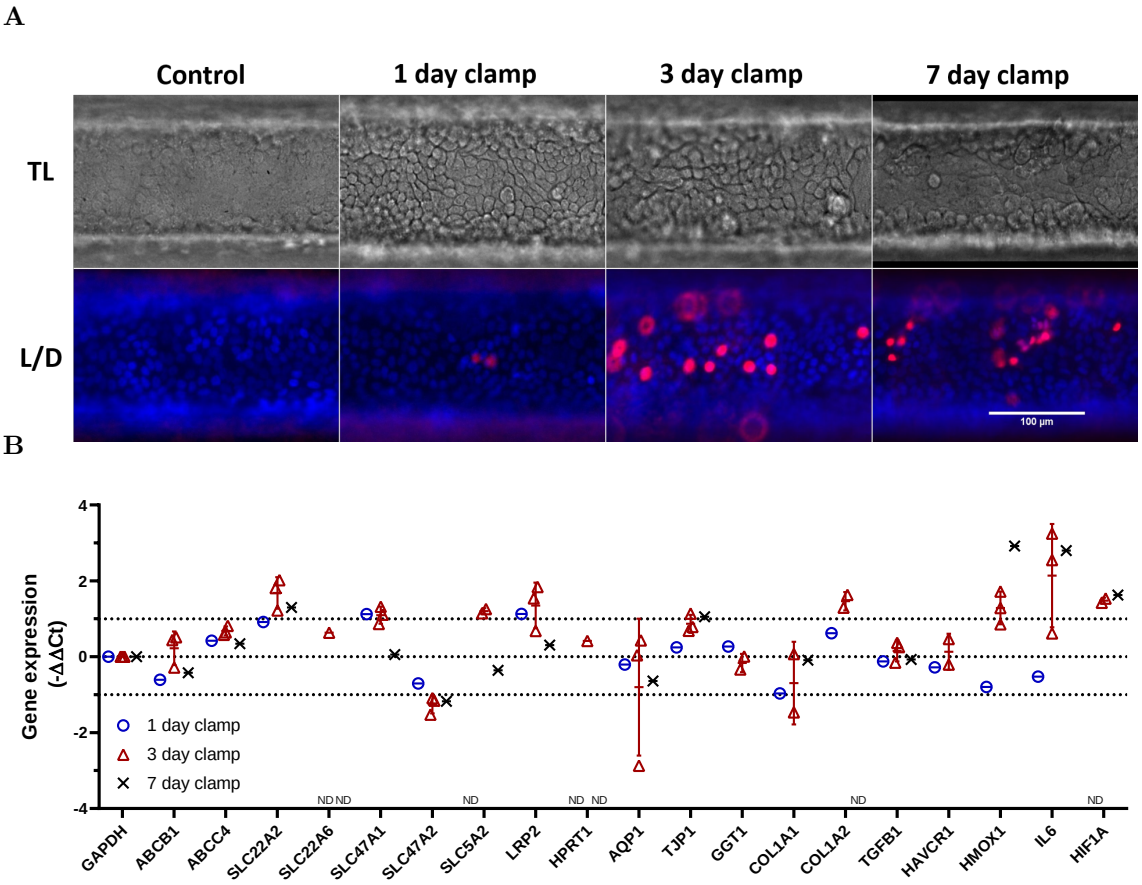

Figure 4.7: Viability and differential gene expression in nutrient and flow deprived (clamped) 3D cultured HRPTEC (1, 3, 7 days) **A.** Representative transmitted light (TL) and Live/Dead (L/D) stain images of 3D cultured HRPTEC. In the L/D stain Live cells can be seen in blue and dead cells can be seen in red. **B.** Gene expression analysis of HRPTEC exposed to clamping treatment for 1, 3 or 7 days compared to unclamped control. Data is presented as mean ± SD of 1 (1 and 7 day clamp) or three (3 day clamp) separate experiments analysed in triplicate (n=1, n=3). Dotted lines represent cut-off value for relevance of differential gene expression (-ΔΔCt <-1 and >1). Expression at 1, 3 or 7 day clamping was normalized against unclamped control, using GAPDH as reference gene to generate -ΔΔCt values. Statistical analysis was performed on 3 day clamping results using separate t-tests, one per gene, Holm-Sidak method was used to correct for multiple comparisons. Genes not evaluated for specific conditions are marked with ND for not determined.

Live/dead staining (Figure 4.7A) of clamped tubes showed no increase in dead cells compared to control after 1 day of clamping. A trend showing an increase in ethidium positive cells can be seen after 3 and 7 days of clamping. Cell count based viability could not be calculated since Live/Dead stain was only performed once for each condition. Differential gene expression did not reveal any significant changes to gene expression, although only the 3 day clamp condition was performed in 3 independent experiments and could be statistically evaluated (Figure 4.7B). Increased expression could be seen for stress markers *COL1A2*, *HMOX1*, *IL6* and *HIF1A* for the 3 day clamp condition, possibly suggesting cell stress. Changes to gene expression after 3 days of clamping can also be seen for drug transporter genes *SLC22A2*, *SLC47A1*, *SLC47A2* and *LRP2* as well as for the glucose transporter gene *SLC5A2*. This may point to initial changes in HRPTEC phenotype in reponse to flow and nutrient deprivation.

5. Discussion & Future studies

The aim of this thesis was to study the effect of flow-related physiological aspects of CKD on drug toxicity in HRPTEC cultured in the Nortis Parvivo system. HRPTEC cultured in 3D displayed increased expression of several proximal tubule drug transporter genes, as well as a reduced expression of renal stress markers in both 5 and 1 week cultures when compared to traditional 2D HRPTEC cultures. 3D cultured cells remained viable for 5 weeks of SFM culture in the Nortis system, at fluid shear stress rates of 0.9 and 1.7 dyne/cm^2. These cultures regained expression of the drug transporter OAT1 and OAT3 detectable in 5 week SFM 3D cultures, indicating a possible novel maturation effect as a result of long term flow culture.

Investigating the effects of increased flow in the Nortis system revealed regained endogenous expression of the drug transporters OAT1 (1 and 5 week cultures) and OAT3 (5 week cultures) in 3D HRPTEC cultures (Figure 4.5), which has not previously been described in literature. Instead, primary HRPTEC have been shown to lose their proximal tubular phenotype, with expression of drug transporters OAT1-4, P-gp and MRP found to be rapidly decreased upon culture.[42] From the results produced in this study it is difficult to establish what the underlying cause of this regained function is as it may be the result of a novel long-term maturation effect or an effect of the use of serum free medium in cultures. To investigate if regained OAT1 and OAT3 expression is associated with a maturation effect of SFM, 5-week Nortis cultures in complete medium could be added to the comparison. Overall, gene expression remained unchanged between flow conditions, indicating no significant changes to cell phenotype in increased fluid shear stress (1.7 dyne/cm^2) treated cells compared to regular fluid shear stress (0.9 dyne/cm^2) treated cells (Figure 4.5). LDH activity also remained unchanged up to 5 weeks in 3D cultured cells exposed to fluid shear stresses of 0.9 dyne/cm^2 and 1.7 dyne/cm^2(Figure 4.3), which does confirm that HRPTEC remain viable in the Nortis system for time periods up to 5 weeks in SFM when exposed to fluid shear stress. In line with what could be seen in 3D HRPTEC cultures, gene expression of drug transporters, PTEC- and cell stress markers in 2D HRPTEC cultures, were unaffected by a fluid shear stress of 1.9 or 5.3 dyne/cm^2 compared to static culture (Figure 4.1). P-gp efflux was also unaffected (Figure 4.2). This goes against what has been shown previously in 2D flow studies using proximal tubule derived cells.[31,37], where significant increase of both P-gp efflux and endocytic uptake function was detected in response to flow treatment. The main reason for these contradictory results could be that the model used in this study differs from the previously mentioned studies in that orbital and not linear flow was used. This difference in the application of flow may have caused an altered cell response compared to what has been observed previously. It should also be mentioned that the presence of primary cilia has not been confirmed in the primary HRPTEC used in this study, which in combination with the results seen in this study puts the flow-sensing ability of these HRPTEC into question.

The phenotype of 3D-cultured HRPTEC was however significantly different compared to 2D cultures and remained stable for up to 5 weeks of culture (Figure 4.6). Most importantly, genes associated with drug transporters the OAT1, OAT3, OCT2, MATE1 and MATE2-K and the endocytosis receptor Megalin were upregulated in 3D cultures.

Expression of OAT3 and upregulation of OCT2 was only detected in 5-week cultures. Downregulation was observed for cell stress markers Collagen I, KIM1 and HO1. This indicates that the HRPTEC phenotype remains stable for up to 5 weeks of culture in SFM, with even a slight improvement compared to 1-week cultures. This difference in phenotype seen when comparing 2D and 3D cultured HRPTEC suggest that the Nortis system is a more suitable model for evaluating proximal tubule drug toxicity compared to 2D culture models and that the serum free culture model used in this study support viable culture for up to 5 weeks. It is however hard to pinpoint what aspect of the chip system causes the changes to cell phenotype between 2D and 3D cultures seen in this study. As both the difference in medium used, presence of flow and ECM in the 3D cultures may all influence the changes to gene expression seen in the transition from 3D to 2D cultures.[37,31,43] It is also important to establish that the differentially expressed drug transporter genes found in this project actually result in changes to cell function. For confirmation of drug transporter expression, transport studies using specific substrates and inhibitors for each upregulated transport gene would have to be optimized for use in the Nortis system. An inconclusive pilot study was run to evaluate BSA-FITC uptake (data not shown) in the 3D cultured cells, suggesting that experimental conditions need to be optimized to accurately evaluate endocytic uptake function in chip cultured cells. Immunofluorescence studies should also be used to identify the localization of drug transporter proteins to establish if their localization in HRPTEC grown in the Nortis system is representative of what is found *in vivo*.[19,20,18,25]

After treatment with the nephrotoxicant polymyxin B at 2 different concentrations (50 or 150 µM) 3D cultured cells displayed a clear toxicity response, showing significant reduction of cell count-based viability and significantly increased levels of LDH activity when treated with 50µM polymyxin B (Figure 4.3,4.4). The toxicity response is consistent with previous studies performed on HRPTEC in the Nortis system, where toxicity was achieved after treatment with 50 and 150 µM of polymyxin B.[35] This suggests that the model used in this study is comparable to other HRPTEC cultures in the Nortis system and that polymyxin B can be used as a positive control for future drug toxicity studies of HRPTEC cultured in the Nortis system. ZO-1 staining of polymyxin B treated cells also indicate that HRPTEC grown in the Nortis system form an epithelial layer throughout the 3D structure, which remains intact after treatment with 50 µM polymyxin B for 48h. These results also confirm that endocytic uptake function is present in HRPTEC cultured in the Nortis system since polymyxin B can only be taken up by the cells by means of endocytosis. However, polymyxin B toxicity does not provide provide a quantitative measurment of endocytic uptake function. To truly evaluate endocytic uptake capacity of chip cultured HRPTEC, BSA-FITC transport studies, similar to the pilot study mentioned previously, would need to be optimized for use in the Nortis system. These results, in combination with the stable (up to 5 weeks) phenotype showing increased expression of drug transporter genes seen in 3D cultured HRPTEC compared to 2D cultured HRPTEC (Figure 4.6), suggest that the Nortis system can be used as tool for long term *in vitro* drug toxicity studies of nephrotoxic compounds. This possibly makes the system a competitive alternative to *in vivo* drug toxicity studies in the future. Suitable testing compounds may include the OAT1 & 3 substrate tenofovir, which is commonly used in the treatment of HIV and chronic Hepatitis B, and has been show to induce proximal tubule toxicity as a result of long term use.[44]

Cells exposed to clamping treatment designed to replicate nutrient deprivation and metabolic stress similar to ischemia displayed a toxicity response after 3 days of clamping. Live/dead

stain showed, a trend towards an increase in dead cells compared to control for both conditions, although no significant changes to gene expression could be detected in HRPTEC exposed to clamping treatment. Some trends suggesting increased expression of renal stress marker and drug transporters can be seen in the 3 day clamping condition. However, no concrete conclusion concerning a possible stress response in the cells can be drawn from the results gained in clamping experiments.

In future studies, it would be necessary to evaluate if the cells used in this study are actually capable of sensing flow. Since no significant change to gene expression in response to flow exposure could be detected in neither 2D nor 3D cultured HRPTEC used in this study. This could be done by evaluating the presence of primary cilia in the cells. This investigation would include immunofluorescence studies, similar to the tight junction protein stain conducted on polymyxin B treated cells in this study, focusing on identifying structural components of primary cilia, along with investigation of signal transduction associated with primary cilia in proximal tubule cells in both the 2D and 3D cell culture models used in this study.

When cultured in the Nortis system, no significant changes to gene expression could be detected in HRPTEC exposed to an increased fluid shear stress. It would therefore be interesting to establish if drug toxicity also remains unchanged in response to increased fluid shear stress. This could be done by complementing the polymyxin B toxicity studies already conducted in this study, with identical experiments conducted at an increased fluid shear stress, replicating the experimental setup used in the differential gene expression evaluation of HRPTEC cultured in the Nortis system, allowing comparison of the toxicity response in the two fluid shear stress conditions.

It would also be relevant to evaluate if the regained gene expression of OAT1 and OAT3 detected in HRPTEC cultured in the Nortis system, is actually represented by protein expression and drug transport function. This would help establish the Nortis system as a more relevant model for drug toxcity studies using antivirals such as tenofovir. A possible approach for this would be to conduct immunofluorescence studies specifically targeting OAT1 and OAT3 in HRPTEC cultured in the Nortis system. This would assist not only in confirming the presence of these transport proteins in the cells but could also be used to determine if the localization of these proteins in cells cultured in the Nortis system is consistent with what can be seen in proximal tubule cells *in vivo*. These immunofluorescence studies could then be complemented with drug transport assays using OAT1 and 3 specific substrates and inhibitors, similar to the Calcein-AM assay conducted on 2D cultured cells in this study, to evaluate if HRPTEC cultured in the Nortis system display OAT1 and OAT3 mediated uptake transport.

6. Conclusions

In this thesis, a cellular stress in response to increased flow treatment and nutrient deprivation could not be conclusively shown in chip cultures, meaning that the aim of creating a model capable of replicating flow related physiological aspects of CKD in the Nortis system could not be achieved under the experimental conditions used for this thesis. HRPTEC cultured in Nortis chips displayed no decrease to cell viability after 5 weeks of culture and regained expression of the drug transporters OAT3 and OAT1, which remained undetectable in 2D cultures. Upregulation of renal drug transporters OCT2, MATE1 and MATE2-K and the endocytosis receptor Megalin was also established in both 1 and 5 week cultures in the Nortis system when compared to 2D cultures. OAT3 and OAT1 are drug transporters responsible for the uptake of antivirals, such as tenofovir, *in vivo*, suggesting that HRPTEC cultured in the Nortis system may provide a proximal tubule model suitable for long term drug toxicity studies of antiviral compounds aimed at treating chronic conditions. In addition, the model could possibly be used as a testing platform for cationic drugs as OCT2 works in conjunction with MATE1/2-K in in the transcellular transfer of organic cations in the proximal tubule. It was also established that HRPTEC grown in the Nortis system display a similar drug toxicity response to polymyxin B as other studies using the same model, indicating that polymyxin B is suitable for use as a positive control for future drug toxicity evaluation in the model. This thesis has thereby shown that 3D HRPTEC Nortis cultures may be more suitable for use in drug toxicity studies compared to static 2D cultures and that mimicking physiology using an MPS system improves HRPTEC phenotype for use in drug toxicity studies. This enables more clinically relevant studies, contributing to drug safety research and ultimately bringing safer drugs to the market.

Bibliography

[1] David Cook, Dearg Brown, Robert Alexander, Ruth March, Paul Morgan, Gemma Satterthwaite, and Menelas N. Pangalos. Lessons learned from the fate of AstraZeneca's drug pipeline: A five-dimensional framework. *Nature Reviews Drug Discovery*, 13(6):419–431, 2014.

[2] Andrew S. Levey and Josef Coresh. Chronic kidney disease. *The Lancet*, 379(9811):165–180, 2012.

[3] Norman P. Curthoys and Orson W. Moe. Proximal tubule function and response to acidosis. *Clinical Journal of the American Society of Nephrology*, 9(9):1627–1638, 2014.

[4] Sanjay K. Nigam, Wei Wu, Kevin T. Bush, Melanie P. Hoenig, Roland C. Blantz, and Vibha Bhatnagar. Handling of drugs, metabolites, and uremic toxins by kidney proximal tubule drug transporters. *Clinical Journal of the American Society of Nephrology*, 10(11):2039–2049, 11 2015.

[5] Walter Boron, Emile Boulpaep, Michael Caplan, Lloyd Cantley, Peter Igarashi, Peter Aronson, and Edward Moczydlowski. *Medical Physiology a Cellular and Molecular Approach*, volume 48. Saunders, 2nd edition, 2009.

[6] Wilhelm Kriz and Birgitte Kaissling. Structural Organization of the Mammalian Kidney. In Robert Alpern, Orson Moe, and Michael Caplan, editors, *Seldin and Giebisch's the Kidney : Physiology and Pathophysiology*, chapter 20, pages 595–693. Elsevier Inc., 5th edition, 2013.

[7] Pedro Caetano-Pinto, Manoe J. Janssen, Linda Gijzen, Laurens Verscheijden, Martijn J.G. Wilmer, and Rosalinde Masereeuw. Fluorescence-Based Transport Assays Revisited in a Human Renal Proximal Tubule Cell Line. *Molecular Pharmaceutics*, 13(3):933–944, 2016.

[8] Elijah J. Weber, Alenka Chapron, Brian D. Chapron, Jenna L. Voellinger, Kevin A. Lidberg, Catherine K. Yeung, Zhican Wang, Yoshiyuki Yamaura, Dale W. Hailey, Thomas Neumann, Danny D. Shen, Kenneth E. Thummel, Kimberly A. Muczynski, Jonathan Himmelfarb, and Edward J. Kelly. Development of a microphysiological model of human kidney proximal tubule function. *Kidney International*, 90(3):627–637, 9 2016.

[9] Bradley M. Denker and Ernesto Sabath. The biology of epithelial cell tight junctions in the kidney. *Journal of the American Society of Nephrology*, 22(4):622–625, 4 2011.

[10] Mariko Hara-Chikuma and A. S. Verkman. Aquaporin-1 facilitates epithelial cell migration in kidney proximal tubule. *Journal of the American Society of Nephrology*, 17(1):39–45, 1 2006.

[11] Venkatesan Raghavan, Youssef Rbaibi, Núria M. Pastor-Soler, Marcelo D. Carattino, and Ora A. Weisz. Shear stress-dependent regulation of apical endocytosis in renal proximal tubule cells mediated by primary cilia. *Proceedings of the National Academy of Sciences of the United States of America*, 111(23):8506–8511, 2014.

[12] Jay N. Pieczynski and Bradley K. Yoder. Renal Cilia Structure, Function, and Physiology. In Robert Alpern, Orson Moe, and Michael Caplan, editors, *Seldin and Giebisch's the Kidney : Physiology and Pathophysiology*, volume 1-2, chapter 11, pages 319–347. Elsevier Inc., 5th edition, 2013.

[13] Shankhajit De, Shoji Kuwahara, and Akihiko Saito. The endocytic receptor megalin and its associated proteins in proximal tubule epithelial cells. *Membranes*, 4(3):333–335, 7 2014.

[14] Akihiko Saito, Hiroyoshi Sato, Noriaki Iino, and Tetsuro Takeda. Molecular mechanisms of receptor-mediated endocytosis in the renal proximal tubular epithelium, 2010.

[15] Pooja Manchandani, Jian Zhou, Jessica T. Babic, Kimberly R. Ledesma, Luan D. Truong, and Vincent H. Tama. Role of renal drug exposure in polymyxin B-induced nephrotoxicity. *Antimicrobial Agents and Chemotherapy*, 61(4), 4 2017.

[16] Hideyuki Motohashi, Yuji Sakurai, Hideyuki Saito, Satohiro Masuda, Yumiko Urakami, Maki Goto, Atsushi Fukatsu, Osamu Ogawa, and Ken Ichi Inui. Gene expression levels and immunolocalization of organic ion transporters in the human kidney. *Journal of the American Society of Nephrology*, 13(4):866–874, 2002.

[17] Hermann Koepsell and Hitoshi Endou. The SLC22 drug transporter family. *Pflugers Archiv European Journal of Physiology*, 447(5):666–676, 2 2004.

[18] Yuko Tanihara, Satohiro Masuda, Tomoko Sato, Toshiya Katsura, Osamu Ogawa, and Ken ichi Inui. Substrate specificity of MATE1 and MATE2-K, human multidrug and toxin extrusions/H+-organic cation antiporters. *Biochemical Pharmacology*, 74(2):359–371, 7 2007.

[19] Kathleen M. Giacomini, Shiew Mei Huang, Donald J. Tweedie, Leslie Z. Benet, Kim L.R. Brouwer, Xiaoyan Chu, Amber Dahlin, Raymond Evers, Volker Fischer, Kathleen M. Hillgren, Keith A. Hoffmaster, Toshihisa Ishikawa, Dietrich Keppler, Richard B. Kim, Caroline A. Lee, Mikko Niemi, Joseph W. Polli, Yuicchi Sugiyama, Peter W. Swaan, Joseph A. Ware, Stephen H. Wright, Sook Wah Yee, MacIej J. Zamek-Gliszczynski, and Lei Zhang. Membrane transporters in drug development. *Nature Reviews Drug Discovery*, 9(3):215–236, 3 2010.

[20] Elaine M. Leslie, Roger G. Deeley, and Susan P.C. Cole. Multidrug resistance proteins: Role of P-glycoprotein, MRP1, MRP2, and BCRP (ABCG2) in tissue defense, 2005.

[21] C. Sauzay, M. White-Koning, I. Hennebelle, T. Deluche, C. Delmas, D. C. Imbs, E. Chatelut, and F. Thomas. Inhibition of OCT2, MATE1 and MATE2-K as a possible mechanism of drug interaction between pazopanib and cisplatin. *Pharmacological Research*, 110:89–95, 8 2016.

[22] James J. Kohler, Seyed H. Hosseini, Elgin Green, Allison Abuin, Tomika Ludaway, Rodney Russ, Robert Santoianni, and William Lewis. Tenofovir renal proximal tubular toxicity is regulated by OAT1 and MRP4 transporters. *Laboratory Investigation*, 91(6):852–858, 6 2011.

[23] Konstantinos Makris and Loukia Spanou. Acute Kidney Injury: Definition, Pathophysiology and Clinical Phenotypes. *The Clinical biochemist. Reviews*, 37(2):85–98, 5 2016.

[24] Yang Dong, Qunzi Zhang, Jiejun Wen, Teng Chen, Li He, Yiyun Wang, Jianyong Yin, Rui Wu, Rui Xue, Shiqi Li, Ying Fan, and Niansong Wang. Ischemic duration and frequency determines AKI-to-CKD progression monitored by dynamic changes of tubular biomarkers in IRI mice. *Frontiers in Physiology*, 10(FEB), 2019.

[25] Manjeri A. Venkatachalam, Joel M. Weinberg, Wilhelm Kriz, and Anil K. Bidani. Failed tubule recovery, AKI-CKD transition, and kidney disease progression. *Journal of the American Society of Nephrology*, 26(8):1765–1776, 8 2015.

[26] Vivekanand Jha, Guillermo Garcia-Garcia, Kunitoshi Iseki, Zuo Li, Saraladevi Naicker, Brett Plattner, Rajiv Saran, Angela Yee Moon Wang, and Chih Wei Yang. Chronic kidney disease: Global dimension and perspectives. *The Lancet*, 382(9888):260–272, 2013.

[27] Rafael Lozano, Mohsen Naghavi, Kyle Foreman, Stephen Lim, Kenji Shibuya, Victor Aboyans, Jerry Abraham, Timothy Adair, Rakesh Aggarwal, Stephanie Y. Ahn, Mohammad A. AlMazroa, Miriam Alvarado, H. Ross Anderson, Laurie M. Anderson, Kathryn G. Andrews, Charles Atkinson, Larry M. Baddour, Suzanne Barker-Collo, David H. Bartels, Michelle L. Bell, Emelia J. Benjamin, Derrick Bennett, Kavi Bhalla, Boris Bikbov, Aref Bin Abdulhak, Gretchen Birbeck, Fiona Blyth, Ian Bolliger, Soufiane Boufous, Chiara Bucello, Michael Burch, Peter Burney, Jonathan Carapetis, Honglei Chen, David Chou, Sumeet S. Chugh, Luc E. Coffeng, Steven D. Colan, Samantha Colquhoun, K. Ellicott Colson, John Condon, Myles D. Connor, Leslie T. Cooper, Matthew Corriere, Monica Cortinovis, Karen Courville De Vaccaro, William Couser, Benjamin C. Cowie, Michael H. Criqui, Marita Cross, Kaustubh C. Dabhadkar, Nabila Dahodwala, Diego De Leo, Louisa Degenhardt, Allyne Delossantos, Julie Denenberg, Don C. Des Jarlais, Samath D. Dharmaratne, E. Ray Dorsey, Tim Driscoll, Herbert Duber, Beth Ebel, Patricia J. Erwin, Patricia Espindola, Majid Ezzati, Valery Feigin, Abraham D. Flaxman, Mohammad H. Forouzanfar, Francis Gerry R. Fowkes, Richard Franklin, Marlene Fransen, Michael K. Freeman, Sherine E. Gabriel, Emmanuela Gakidou, Flavio Gaspari, Richard F. Gillum, Diego Gonzalez-Medina, Yara A. Halasa, Diana Haring, James E. Harrison, Rasmus Havmoeller, Roderick J. Hay, Bruno Hoen, Peter J. Hotez, Damian Hoy, Kathryn H. Jacobsen, Spencer L. James, Rashmi Jasrasaria, Sudha Jayaraman, Nicole Johns, Ganesan Karthikeyan, Nicholas Kassebaum, Andre Keren, Jon Paul Khoo, Lisa Marie Knowlton, Olive Kobusingye, Adofo Koranteng, Rita Krishnamurthi, Michael Lipnick, Steven E. Lipshultz, Summer Lockett Ohno, Jacqueline Mabweijano, Michael F. MacIntyre, Leslie Mallinger, Lyn March, Guy B. Marks, Robin Marks, Akira Matsumori, Richard Matzopoulos, Bongani M. Mayosi, John H. McAnulty, Mary M. McDermott, John McGrath, Ziad A. Memish, George A. Mensah, Tony R. Merriman, Catherine Michaud, Matthew Miller, Ted R. Miller, Charles Mock, Ana Olga Mocumbi, Ali A. Mokdad, Andrew Moran, Kim Mulholland, M. Nathan Nair, Luigi Naldi, K. M.Venkat Narayan, Kiumarss Nasseri, Paul Norman, Martin O'Donnell, Saad B. Omer, Katrina Ortblad, Richard Osborne, Doruk Ozgediz, Bishnu Pahari, Jeyaraj Durai Pandian, Andrea Panozo Rivero, Rogelio Perez Padilla, Fernando Perez-Ruiz, Norberto Perico, David Phillips, Kelsey Pierce, C. Arden Pope, Esteban Porrini, Farshad Pourmalek, Murugesan Raju, Dharani Ranganathan, Jürgen T. Rehm, David B. Rein, Guiseppe Remuzzi, Frederick P. Rivara, Thomas Roberts, Felipe Rodriguez De León, Lisa C. Rosenfeld, Lesley Rushton, Ralph L. Sacco, Joshua A. Salomon, Uchechukwu Sampson, Ella Sanman, David C. Schwebel, Maria Segui-Gomez, Donald S. Shepard, David Singh, Jessica Singleton, Karen Sliwa, Emma Smith, Andrew Steer, Jennifer A. Tay-

lor, Bernadette Thomas, Imad M. Tleyjeh, Jeffrey A. Towbin, Thomas Truelsen, Eduardo A. Undurraga, N. Venketasubramanian, Lakshmi Vijayakumar, Theo Vos, Gregory R. Wagner, Mengru Wang, Wenzhi Wang, Kerrianne Watt, Martin A. Weinstock, Robert Weintraub, James D. Wilkinson, Anthony D. Woolf, Sarah Wulf, Pon Hsiu Yeh, Paul Yip, Azadeh Zabetian, Zhi Jie Zheng, Alan D. Lopez, and Christopher J.L. Murray. Global and regional mortality from 235 causes of death for 20 age groups in 1990 and 2010: A systematic analysis for the Global Burden of Disease Study 2010. *The Lancet*, 380(9859):2095–2128, 12 2012.

[28] Imed Helal, Godela M. Fick-Brosnahan, Berenice Reed-Gitomer, and Robert W. Schrier. Glomerular hyperfiltration: Definitions, mechanisms and clinical implications. *Nature Reviews Nephrology*, 8(5):293–300, 5 2012.

[29] Avry Chagnac, Boris Zingerman, Benaya Rozen-Zvi, and Michal Herman-Edelstein. Consequences of glomerular hyperfiltration: The role of physical forces in the pathogenesis of chronic kidney disease in diabetes and obesity. *Nephron*, 143(1):38–42, 2019.

[30] Lu Ping Li, Huan Tan, Jon M. Thacker, Wei Li, Ying Zhou, Orly Kohn, Stuart M. Sprague, and Pottumarthi V. Prasad. Evaluation of Renal Blood Flow in Chronic Kidney Disease Using Arterial Spin Labeling Perfusion Magnetic Resonance Imaging. *Kidney International Reports*, 2(1):36–43, 1 2017.

[31] Kyung Jin Jang, Ali Poyan Mehr, Geraldine A. Hamilton, Lori A. McPartlin, Seyoon Chung, Kahp Yang Suh, and Donald E. Ingber. Human kidney proximal tubule-on-a-chip for drug transport and nephrotoxicity assessment. *Integrative Biology (United Kingdom)*, 5(9):1119–1129, 2013.

[32] Tom T.G. Nieskens and Martijn J. Wilmer. Kidney-on-a-chip technology for renal proximal tubule tissue reconstruction. *European Journal of Pharmacology*, 790:46–56, 2016.

[33] Yasunori Fukuda, Misato Kaishima, Toshiyuki Ohnishi, Kimio Tohyama, Ikumi Chisaki, Yusuke Nakayama, Mari Ogasawara-Shimizu, and Yuji Kawamata. Fluid shear stress stimulates MATE2-K expression via Nrf2 pathway activation. *Biochemical and Biophysical Research Communications*, 484(2):358–364, 2017.

[34] Courtney Sakolish, Elijah J. Weber, Edward J. Kelly, Jonathan Himmelfarb, Roula Mouneimne, Fabian A. Grimm, John S. House, Terry Wade, Arum Han, Weihsueh A. Chiu, and Ivan Rusyn. Technology Transfer of the Microphysiological Systems: A Case Study of the Human Proximal Tubule Tissue Chip. *Scientific Reports*, 8(1):1–14, 2018.

[35] Elijah J. Weber, Kevin A. Lidberg, Lu Wang, Theo K. Bammler, James W. MacDonald, Mavis J. Li, Michelle Redhair, William M. Atkins, Cecilia Tran, Kelly M. Hines, Josi Herron, Libin Xu, Maria Beatriz Monteiro, Susanne Ramm, Vishal Vaidya, Martti Vaara, Timo Vaara, Jonathan Himmelfarb, and Edward J. Kelly. Human kidney on a chip assessment of polymyxin antibiotic nephrotoxicity. *JCI insight*, 3(24), 2018.

[36] Joanne Y.C. Soo, Jitske Jansen, Rosalinde Masereeuw, and Melissa H. Little. Advances in predictive in vitro models of drug-induced nephrotoxicity. *Nature Reviews Nephrology*, 14(6):378–393, 2018.

[37] Jelle Vriend, Janny G.P. Peters, Tom T.G. Nieskens, Renata Škovroňová, Nina Blaimschein, Miriam Schmidts, Ronald Roepman, Tom J.J. Schirris, Frans G.M. Russel,

Rosalinde Masereeuw, and Martijn J. Wilmer. Flow stimulates drug transport in a human kidney proximal tubule-on-a-chip independent of primary cilia. *Biochimica et Biophysica Acta - General Subjects*, 1 2019.

[38] Thomas Ludwig, Christoph Riethmüller, Michael Gekle, Gerald Schwerdt, and Hans Oberleithner. Nephrotoxicity of platinum complexes is related to basolateral organic cation transport. *Kidney International*, 66(1):196–202, 2004.

[39] Christian Maass, Nathan B. Sorensen, Jonathan Himmelfarb, Edward J. Kelly, Cynthia L. Stokes, and Murat Cirit. Translational Assessment of Drug-Induced Proximal Tubule Injury Using a Kidney Microphysiological System. *CPT: Pharmacometrics and Systems Pharmacology*, 8(5):316–325, 5 2019.

[40] Nicholas Ferrell, Ruben M. Sandoval, Bruce A. Molitoris, Paul Brakeman, Shuvo Roy, and William H. Fissell. Application of physiological shear stress to renal tubular epithelial cells. In Thomas Weimbs, editor, *Methods in Cell Biology*, volume 153, chapter 3, pages 43–67. Elselvier Inc., 1st edition, 2019.

[41] Nicholas Ferrell, Jin Cheng, Simeng Miao, Shuvo Roy, and William H. Fissell. Orbital shear stress regulates differentiation and barrier function of primary renal tubular epithelial cells. *ASAIO Journal*, 64(6):766–772, 2018.

[42] Colin D.A. Brown, Rachel Sayer, Amy S. Windass, Iain S. Haslam, Marc E. De Broe, Patrick C. D'Haese, and Anja Verhulst. Characterisation of human tubular cell monolayers as a model of proximal tubular xenobiotic handling. *Toxicology and Applied Pharmacology*, 233(3):428–438, 2008.

[43] M. J. Bissell and M. H. Barcellos-Hoff. The influence of extracellular matrix on gene expression: is structure the message? *Journal of Cell Science*, 1987(SUPPL. 8):327–343, 3 1987.

[44] Sana Waheed, Doaa Attia, Michelle M. Estrella, Yousuf Zafar, Mohamed G. Atta, Gregory M. Lucas, and Derek M. Fine. Proximal tubular dysfunction and kidney injury associated with tenofovir in HIV patients: A case series. *Clinical Kidney Journal*, 8(4):420–425, 2015.

References of figures

[1] CNX Openstax 2016, 'Biology', Wikimedia Commons. Accessed: 2020-01-21.
URL: *https://commons.wikimedia.org/wiki/File:Figure_41_03_04.jpg*

[2] ColnKurtz 2017, 'Acute renal failure', Wikimedia Commons. Accessed: 2020-01-21.
URL: *https://commons.wikimedia.org/wiki/File:Acute_Renal_Failure.svg*

[3] Nortis, Inc. 2019, 'The ParVivo™ Organ-on-Chip Platform', Marketing presentation. Accessed: 2019-12-21.

DEPARTMENT OF PHYSICS
CHALMERS UNIVERSITY OF TECHNOLOGY
Gothenburg, Sweden
www.chalmers.se

CHALMERS
UNIVERSITY OF TECHNOLOGY